Electromagnetic geothermal exploration in the Netherlands

review of the CSEM and MT methods

Report by SCAN

December 2019

Ministerie van Economische Zaken en Klimaat
ebn
TNO
Interreg North-West Europe DGE-ROLLOUT

This page intentionally left blank

Electromagnetic geothermal exploration in the Netherlands

review of the CSEM and MT methods

Report written by Wouter van Leeuwen (IF Technology)

December 2019

Dit rapport is een product van het SCAN-programma en wordt mogelijk gemaakt door het Ministerie van Economische Zaken en Klimaat

Table of Contents

Samenvatting

Doelstellingen

Het belangrijkste doel van deze review is onderzoeken in hoeverre de magnetotellurische methode (MT) en controlled source elektromagnetisme (CSEM) geschikt zijn voor geothermische exploratie in Nederland.

Door aan het aardoppervlak de tijdsvariaties in het elektromagnetische veld te meten, worden met behulp van de magnetotellurische methode (MT) en controlled source elektromagnetisme (CSEM) de elektrische weerstandsstructuren van de ondergrond in beeld gebracht. Aangezien een lage elektrische weerstand een mogelijke indicatie is voor het voorkomen van geothermisch water (porositeit), geeft het resulterende model informatie over het bestudeerde geothermische reservoir. De technische mogelijkheden en kosten van het toepassen van MT en CSEM voor de exploratie van geothermische reservoirs in Nederland kende voorafgaand aan deze studie nog veel onzekerheden. Dit is mede veroorzaakt door het ontbreken van een gedegen analyse van relevante voorbeeldprojecten in vergelijkbare omstandigheden en het ontbreken van een gestructureerd en doelgericht onderzoek hiernaar. Om deze onzekerheden te verkleinen en een zo goed mogelijke uitspraak over de mogelijkheden van MT en CSEM voor geothermische exploratie te kunnen doen, worden in deze studie een aantal voorbeeldprojecten geanalyseerd. Daarnaast wordt een generieke projectdoorloop van een EM project gepresenteerd en besproken, inclusief een ruwe inschatting van de verwachte kosten van een elektromagnetische data acquisitie survey. Om een inschatting te kunnen maken van de toepasbaarheid van MT en CSEM in Nederland, zijn de antwoorden op verschillende deelvragen gezocht.

Aangezien Nederland dicht bebouwd is en veel infrastructuur kent, is het de verwachting dat elektromagnetische signalen verstoord zullen worden door “ruis”. Aan de hand van een in 2015 gemeten dataset in de Noordoostpolder wordt bekeken in welke mate deze ruis de kwaliteit van de gemeten data negatief beïnvloedt. Dit heeft invloed op de maximale diepte tot waar elektromagnetische methodes kunnen meten.

Het is bekend dat de Nederlandse ondergrond weinig contrast in elektrische weerstand bevat, dit heeft grote invloed op de resolutie en het onderscheidend vermogen van de technieken. Aan de hand van enkele voorbeeldprojecten wordt bekeken wat verwacht kan worden van MT en CSEM in de Nederlandse situatie.

Conclusies

De belangrijkste conclusie uit dit onderzoek is dat er op dit moment geen goed voorbeeld beschikbaar is om een algemene uitspraak te doen over de toepasbaarheid van CSEM en MT voor alle geothermische exploratie in Nederland. Daarnaast zijn beide methoden geen vervangende maar aanvullende technieken voor seismische data. De toegevoegde waarde ten opzichte van seismische data is te vinden in de lagere acquisitiekosten en de mogelijkheid om de gemeten elektrische weerstand direct aan porositeit te correleren. Hiernaast kunnen meerdere deelconclusies getrokken worden.

- MT en CSEM bieden weinig meerwaarde ten opzichte van seismische data om de formaties van de Boven en Midden Noordzee Groep in beeld te brengen.
- In Nederland is met het ontbreken van magmatisch water en het voorkomen van de daaraan gerelateerde klei alteratie mineralen een belangrijke factor voor het succesvol toepassen van MT voor het exploreren van geothermische reservoirs afwezig.

- Op basis van de experimenten in Luttelgeest en België lijkt een dieptepenetratie van ongeveer 2 km haalbaar met MT en CSEM.
- Op basis van de beschikbare gegevens lijkt het mogelijk om goede kwaliteit MT data te acquireren in rurale gebieden met weinig EM ruis als gevolg van bebouwing en infrastructuur.
- Op basis van de meetresultaten van de MT pilot en het EM experiment bij Luttelgeest is geconstateerd dat de impact op de signaalkwaliteit van het DC spoorwegnetwerk in NL kleiner is dan verwacht.
- De beste CSEM resultaten worden behaald wanneer gebruik wordt gemaakt van meerdere elektrische injectiebronnen rondom het onderzoeksgebied met een maximale afstand tussen bron en ontvanger van ongeveer 4 km.
- Informatie en data van seismiek en putten dienen gebruikt te worden tijdens alle fases van het modelleren (pre- en post-survey).
- Gezien de relatieve kleinschaligheid en beperkte impact, kan een MT en/of CSEM survey eenvoudig georganiseerd worden in het kielzog van een seismische acquisitie campagne.

Aanbevelingen

Om tot de beste inschatting van de toepasbaarheid van MT en/of CSEM in Nederland te komen is het aan te bevelen om een gestructureerd en voldoende gesubsidieerd veldonderzoek uit te voeren op een relevante locatie in Nederland binnen bijvoorbeeld een post-doc of PhD-thesis onderzoek en/of in combinatie met lopende / aanstaande seismische campagnes. Tot op heden is dit nog niet gebeurd. Verder zou het aanzienlijk helpen wanneer de data gemeten door VITO in België in 2017 beschikbaar wordt gemaakt voor nadere analyse. Daarnaast zijn de volgende praktische aanbevelingen bepaald:

- Weet wat je meet. Bepaal vooraf of je je doelreservoir kan meten met EM data, voorwaarde daarvoor is een meetbaar elektrische weerstandscontrast tussen het doelreservoir en het omringende gesteente. Om dit te bepalen dient een synthetisch model van de ondergrond gemaakt te worden, zodat de optimale survey parameters kunnen worden bepaald. Gebruik hierbij bestaande data en informatie van putten en seismiek. Het inzichtelijk maken van welke structuren onderscheiden kunnen gaan worden en welke acquisitieparameters daaraan bijdragen zijn cruciaal voor een succesvolle campagne.
- Pre-survey scouting voor geschikte meetlocaties en goede communicatie met landeigenaren is essentieel voor het vergaren van goede kwaliteit data.
- Vermijd dichtbebouwd, stedelijk gebied. Plan een meetstation op tenminste één kilometer van een DC spoorlijn.
- Voor de beste meetresultaten is een pragmatische houding belangrijk. Blijf in nauw contact met de veldploeg en gebruik duidelijke procedures.
- Neem tijdens het processen de tijd om verschillende strategieën te testen. Gezien de aanwezigheid van EM ruis en de ondergrond met beperkt contrast, is een weloverwegen data processing fase in Nederland noodzakelijk.
- Om tot het meest accurate en betrouwbare ondergrondmodel te komen, is het verstandig om geologische randvoorwaarden te gebruiken tijdens inversie modellering van de gemeten data.

Summary

Objectives

The main objective of this review is to investigate if the magnetotelluric method (MT) and controlled-source electromagnetics (CSEM) can be successfully applied for geothermal exploration in the Netherlands.

By measuring the time-variations in the Earth's electromagnetic field, the subsurface resistivity structure of the subsurface can be imaged using MT and CSEM. The presence of geothermal water (porosity) is indicated by a low electrical resistance. Consequently, the resulting resistivity model provides information on the studied geothermal reservoir. Prior to this study, many uncertainties existed about the technical possibilities and costs for deploying MT and CSEM for geothermal exploration in the Netherlands. The absence of an analyses of relevant case studies and the lack of a structured research on the subject are mainly responsible for this knowledge gap. In this study, several case studies are analyzed to decrease these uncertainties and provide an as conclusive as possible statement regarding the feasibility of MT and CSEM for geothermal exploration. Additionally, a general project workflow is presented which includes a rough estimate of the necessary budget for an electromagnetic survey. To arrive at a meaningful statement regarding the feasibility of MT and CSEM in the Netherlands, the following sub questions are investigated.

As the Netherlands is a heavily urbanized country with abundant infrastructure, it is expected that the electromagnetic signals will be disturbed by noise. The impact of this EM noise on the data quality of the measured signal is analyzed on the basis of a data set acquired in 2017 in the Noordoostpolder. It is expected that the impact of noise on the data mainly influences the maximum penetration depth of the electromagnetic methods.

It is known that the subsurface of the Netherlands bears small contrasts in electrical resistivity. This has a major influence on the resolution and the resolving capabilities of the methods studied. By studying several case studies it is estimated what can be expected from MT and CSEM given the composition of the subsurface of the Netherlands.

Conclusions

As no representative case studies are available it is not possible to formulate an overall conclusive statement regarding the feasibility of CSEM and MT for geothermal exploration in the Netherlands. Both methods provide additional data for subsurface information and are not an alternative for seismic data. When compared to seismic data, the added value of the EM methods are the lower data acquisition costs and the possibility to directly relate electrical resistivity to porosity. Furthermore, several smaller conclusions are formulated.

- MT and CSEM offer limited potential to image the formation of the Upper and Middle North Sea Groups.
- The absence of magmatic waters and related clay alteration minerals in the Netherlands implies that an important factor for successfully applying MT for geothermal exploration is missing.
- The experiments in Luttelgeest (Noordoostpolder) and Belgium proved that with the EM method you can measure up to a depth of about 2 km below the surface.
- The experiments in Luttelgeest and Belgium proved that acquiring good quality EM data in Belgium and the Netherlands is possible, despite the numerous EM noise sources.

- The experiment in Luttelgeest showed that impact of the DC railway network on the data quality is much smaller than anticipated.
- Optimal CSEM data acquisition results are expected when two or three dipoles are located around a survey area with a maximum source receiver distance of about 4 km.
- The synthetic experiments showed that when modelling, information from wells and seismic data should be used to build realistic subsurface resistivity models.
- As an MT and/or CSEM survey is relatively small, it can be organized in parallel with a seismic acquisition campaign.

Recommendations

In order to be able to formulate an overall conclusive statement regarding to the applicability of MT and/or CSEM in the Netherlands it is recommended to carry out a structured and sufficiently funded field research at a relevant location in the Netherlands. A post-doc or PhD-thesis research and/or the combination with running or scheduled seismic campaigns would be a good opportunity to achieve this. Until this day, such a research has not been carried out in the Netherlands. A valuable extra source of information is the EM data measured by VITO in Belgium in 2017, making this data available for further analysis will impact the conclusiveness of the project significantly. Furthermore, the following is recommended:

- Know what you measure. Choose a target that can be detected in the electromagnetic data; a detectable resistivity contrast between the target and the surrounding rocks should be present. To do this, make synthetic models to predict the subsurface response and determine to optimal survey parameters and layout. Use existing knowledge and data (seismic and well data) from the subsurface. Gaining insight in which subsurface structures can be imaged and which acquisition parameters contribute to the objective of the survey are crucial for a successful campaign.
- Pre-survey scouting for suitable station locations and good communications with land owners is essential to acquire good quality data.
- Stay away from urbanized areas when planning a survey. Don’t plan a station location too close to a DC railway line.
- In the field, plan and be pragmatic to obtain the best survey results. Stay on top of your crew. Solid field procedures are very important for good quality data.
- During processing, take time and test various processing strategies. Due to the presence of EM-noise and the subsurface conditions, thoughtful processing is necessary in the Netherlands.
- During inversion modelling, use geological constraints from existing subsurface models and well log data to guide the inversion modelling. This increases the accuracy and reliability of the resulting subsurface model.
- As the electromagnetic response measured is a volumetric measurement, more reliable results are obtained by 3-D models. The validity structures observed in the 3-D model can be tested by stitched or interpolated 1-D models.

Introduction

Geothermal energy systems have been considered as a potential alternative for the fossil energy use. Currently, geothermal projects are already in use in the Netherlands. However, the application of geothermal energy in existing projects is not adequate for the provision of high temperature heat for, as an example, the process industry. It is anticipated that Ultra Deep Geothermal (UDG) energy could potentially make a substantial contribution to the transition towards a sustainable energy supply. To reach sufficiently high temperatures (>130°C) in the Netherlands, geothermal reservoirs at depths of over 4 km are required. The Dutch subsurface at these depths has not been explored extensively until now and is therefore relatively unknown. Based on the limited amount of subsurface data, the Lower Carboniferous (Dinantian) carbonates were identified by Boxem et al. (2016) as the most promising target matching the initial requirements for UDG.

The study reported in this document is a result of SCAN, a government funded program to scope out the potential of geothermal energy, including the Dinantian carbonates. This program includes a range of subsurface studies of the Dinantian carbonates. The results of the SCAN studies will be released and become available via www.nlog.nl.

Although, electromagnetic methods cover a broad range of techniques and sounding depths, this review document only covers onshore Controlled-Source Electromagnetics (CSEM) and Magnetotellurics (MT). The reason for this choice is that CSEM and MT are the two methods that might have potential for geothermal exploration in the Netherlands. Other electromagnetic methods generally have insufficient penetration depth to image the deep subsurface. The difference between MT and CSEM is the nature of the source signal. MT is a passive method which utilizes the time variations caused by solar activity and global lightning to image the electrical resistivity structure of the subsurface. CSEM is an active method which utilizes the time variations of an electrical current injected into the subsurface to image the electrical resistivity structure of the subsurface. Generally, MT has the ability to measure deeper structures, where CSEM is less sensitive to external electromagnetic noise.

Where MT is a proven exploration tool for medium and high enthalpy geothermal systems related to volcanic activity, it's feasibility for deep geothermal exploration (> 500 m b.m.s.l[1]) in the Netherlands is uncertain. In this study the feasibility of MT as a geothermal exploration method is explored on the basis of literature, published case studies and an actual pilot survey conducted in 2017 near Luttelgeest, the Netherlands.

Where offshore CSEM is a proven technique which is generally applied for hydrocarbon exploration purposes (Constable, 2010; Constable and Srnka, 2007), the potential of CSEM for onshore geothermal exploration is a relatively recent research topic. Due to the limited experience, it's actual potential is not yet well described. A few examples for geothermal exploration and carbon capture storage monitoring are known and are reviewed in this study, while an actual pilot survey conducted in the Netherlands was carried out in order to gain insight in the onshore potential of CSEM as an exploration tool.

This study focusses on answering the question whether or not MT and CSEM methods can be successfully deployed for geothermal exploration in the Netherlands. In this sense, it concentrates not only on deep, unconventional geothermal aquifers, such as the Dinantian Carbonates, but also on more shallow, already developed geothermal reservoirs such as, for

[1] Below Mean Sea Level

example, the Slochteren Formation. Subsequent topics addressed in this study are the following.

The expected depth of penetration of electromagnetic methods

As the Dutch subsurface mainly consists of conductive sedimentary layers, it is expected that the electromagnetic signal will have difficulties penetrating to depths greater than four kilometre. As the strength of the source is a limiting factor, CSEM measurements will have a shallower depth of penetration in comparison to MT measurements.

The expected structures and properties imaged by electromagnetic methods

The propagation of the electromagnetic field is diffusive, therefore its resolving power depends on the dimensions of the target, as well as its resistivity contrast with respect to the background resistivity. The resolving power of electromagnetic methods can be improved by adding a priori geological constraints to the model.

Due to the nature of the Dutch subsurface, only small resistivity contrasts are present. Main topics researched with respect to this topic is whether or not faults and porous geological structures can be detected by electromagnetic methods. In general CSEM is better in resolving resistive anomalies while MT is better in resolving conductive anomalies.

The influence of man-made noise in urban areas on the electromagnetic signal

It is known that electric motors, power cables, buried pipes, trains, and other human activity disturb the electromagnetic signal. As the Netherlands is densely populated, it is investigated on the basis of actual data, how heavily human activity influences the measured electromagnetic signal. To this end, data and information from two experiments conducted in the Netherlands and one experiment conducted in Belgium are used.

Besides these two fundamental topics, a best practice workflow for MT and CSEM in the Netherlands is proposed. This workflow is based on the experience with electromagnetic methods in the Netherlands and analogue survey environments and considers the aim of the survey, the method used, the Dutch landscape and subsurface, planning and budgeting.

After introducing the current state of the art of MT and CSEM in geothermal exploration in the Netherlands and abroad, a CSEM-MT experiment conducted around Luttelgeest is presented. Following, the main theoretical framework of the two methods is described. The next two chapters are dedicated to best practices in data acquisition, processing and modelling of both MT and CSEM data. First, the general workflow of an EM survey is introduced, after which, on basis of real case examples, best practices for EM geothermal exploration in the Netherlands are proposed. Ultimately, the main learning and findings regarding the applicability of MT and CSESM for geothermal exploration in the Netherlands are summarized.

Electromagnetic methods

Electromagnetic theory

Magnetotellurics is a non-invasive geophysical technique which utilizes the time variations of the Earth's electromagnetic fields to image the electrical resistivity structure of the subsurface. Magnetotellurics is utilized for research purposes and commercial activities such as deep crustal studies and mining exploration. Besides these applications, magnetotellurics has a long track record in the exploration of convection-dominated play type geothermal systems. This is especially the case for volcanic type geothermal systems, which have a clear resistivity pattern (Manzella et al., 2006; Pellerin et al., 1996; Spichak and Manzella, 2009). Controlled-source electromagnetics (CSEM) is also a non-invasive geophysical technique, but in contrast to magnetotellurics, it is utilizing the electromagnetic field of an induced source to image the resistivity structure of the subsurface. Marine CSEM is generally applied for hydrocarbon exploration (Constable, 2010; Streich, 2015). Land CSEM applications are relatively recent and besides hydrocarbon exploration and monitoring, examples are known from CO_2 sequestration storage monitoring and geothermal exploration (Schaller et al., 2018; Streich, 2015; Streich et al., 2013).

This section is a summary derived from van Leeuwen (2016) and, where necessary, complemented with controlled-source electromagnetic specific aspects.

Magnetotellurics and controlled-source electromagnetics

During an electromagnetic experiment the time-variations of the electromagnetic fields of the Earth are measured to determine the electrical resistivity structure of the subsurface. The electric response of the Earth's subsurface can be obtained from large depths by extending the measuring (or sounding) period during a magnetotelluric experiment. This principle is described in the electromagnetic skin depth relation, which is in a simplified form (Spies, 1989):

$$p(T) \approx 500\sqrt{T}\rho_a.$$

Here $p(T)$ is the electromagnetic skin depth in metre [m], T is the magnetotelluric sounding period in seconds [s] and ρ_a is the apparent resistivity in Ohm-metre [Ωm].

Bulk electrical resistivity of Earth's materials present in the crust and upper mantle are ranging from 10^{-1} to 10^5 Ωm. Magnetotelluric experiments are typically conducted in the frequency range from 10^{-4} to 10^5 s (Chave and Jones, 2012). Taking this into account, the skin depth of a magnetotelluric experiment ranges from several tens of meters to several hundreds of kilometres, or in other words from the near-surface deep into the Earth's mantle.

The variations of the Earth's electromagnetic fields measured during a magnetotelluric sounding are initiated by lightning discharges or interactions between solar plasma and the ionosphere and magnetosphere. Here the former is causing high frequency (≥ 10 Hz) time variations and the latter is causing low frequency (≤ 10 Hz) time variations (Simpson and Bahr, 2005). A more detailed description of the sources inducing the time-variations in the electromagnetic fields can for example be found in Chave and Jones (2012). In contrast to the natural source utilized by magnetotellurics, controlled source electromagnetics utilizes the time-variations in the electromagnetic fields of an artificial source to determine the resistivity structure of the subsurface.

The relationship between electrical and magnetic fields in a medium is described by the Maxwell equations. Assuming linear constitutive relationships in the material properties of the medium and considering that time-varying displacement currents are negligible, electric and magnetic fields can be related through the constitutive equations. Furthermore, considering an isotropic medium, i.e. electric permittivity and electrical conductivity are all scalars, as well as assuming a free space
magnetic permeability, a set of Maxwell equations becomes available which can be used for a wide range of geophysical problems including magnetotellurics and controlled source electromagnetics (Chave and Jones, 2012).

In the following some important relevant concepts in relation to electromagnetic methods are discussed. Most of the text is slightly modified or taken from van Leeuwen (2016). Although the context is the magnetotelluric method, these concepts are also valid for CSEM, unless discussed otherwise.

Transfer function

Assuming a time-varying quasi-uniform horizontal magnetic field above the surface of the Earth, inducing an electric field within the Earth, the relation between the electric and magnetic fields at the surface of the Earth can be described by the magnetotelluric transfer function Z [V A^{-1}]:

$$\bar{E}_h = \bar{\bar{Z}} \cdot \bar{B}_h,$$

where $\bar{E}_h$ [Vm^{-1}] and $\bar{B}_h$ [Vm^{-1}] are the horizontal electric and magnetic fields in the spectral domain. The magnetotelluric transfer function is the ultimate target during am electromagnetic survey. It is estimated from the measured horizontal electric and magnetic fields.

By assuming an isotropic earth, with respect to the variations in the electrical resistivity, negligible variations in the magnetic permeabilities and electrical permittivities, as well as negligible displacement current with the respect to measurement periods, a homogeneous half space and no current source within the earth, equations can be derived for the relations between all horizontal electromagnetic field directions which leads to the definition of the magnetotelluric transfer function:

$$\begin{bmatrix} E_x \\ E_y \end{bmatrix} = \begin{bmatrix} Z_{xx} & Z_{xy} \\ Z_{yx} & Z_{yy} \end{bmatrix} \cdot \begin{bmatrix} B_x \\ B_y \end{bmatrix}.$$

Since in a 2-D case $Z_{xx} = Z_{yy} = 0$ and considering, the horizontal electric and magnetic fields for a uniform half-space can be related as:

$$\rho_a(\omega) = \mu_0 \omega |C|^2,$$

where ρ_a is the apparent resistivity, μ_0 is the free-space value of the magnetic permeability ($\mu_0 = 1.2566 \times 10^{-6}\ Hm^{-1}$), ω [s^{-1}] is the angular frequency, and C [km] is the Smucker-Weidelt C-response ($C = \frac{E_x}{i\omega B_y}$).

Similarly, for a CSEM experiment the relation between the recorded electric field $\bar{E}$, and the injected source waveform $\bar{I}_k$, is described by the transfer function $\bar{\bar{T}}_k^E$ [A/m^2]:

$$\bar{E} = \bar{\bar{T}}_k^E \cdot \bar{I}_k.$$

For a dipole configuration and including the magnetic field responses, this equation can be rewritten into the relation between the source currents and the EM field in matrix form (Streich et al., 2013):

$$\begin{bmatrix} E_x \\ E_y \\ H_x \\ H_y \\ H_z \end{bmatrix} = \begin{bmatrix} T_{1,3}^{E_x} & T_{2,3}^{E_x} \\ T_{1,3}^{E_y} & T_{2,3}^{E_y} \\ T_{1,3}^{H_x} & T_{2,3}^{H_x} \\ T_{1,3}^{H_y} & T_{2,3}^{H_y} \\ T_{1,3}^{H_z} & T_{2,3}^{H_z} \end{bmatrix} \cdot \begin{bmatrix} I_1 \\ I_2 \end{bmatrix}.$$

In contrast to the magnetotelluric transfer function, the amplitudes of the transfer functions here are expressed as current density in A/m^2.

Tipper

Similar to the transfer function, a relationship between the horizontal and vertical magnetic fields can be formulated as:

$$B_z = \bar{T} \cdot \bar{B}_h,$$

where B_z is the vertical magnetic field and $\bar{T}$ [V A^{-1}] is the vertical magnetic transfer function, or Tipper.

Similar to the magnetotelluric transfer function, an equation can be derived for the Tipper:

$$B_z = \begin{bmatrix} T_{zx} \\ T_{zy} \end{bmatrix} \cdot \begin{bmatrix} B_x \\ B_y \end{bmatrix}.$$

Dimensionality

Dimensionality distortions in the electromagnetic signal are caused by 2-D or 3-D structures in the subsurface and will be reflected in the chosen survey design and modelling strategy. Care should be taken when the dimensionality of the structures in the subsurface is different from the dimensionality of the modelling code used. In those instances, inaccurate resistivity structures might be resolved by the modelling, leading to an erroneous geological interpretation of the inversion model. Independent of the dimensionality of the data, the main resistivity structures resolved by either 1-D, 2-D and 3-D inversions are all credible (Ledo et al., 2002). To illustrate this, a resistivity cross-section resulting from 1-D, 2-D and 3-D inversions of magnetotelluric data acquired in the Glass Mountain geothermal field in the USA is shown in Figure 1. In Figure 1 it can be observed that although the main resistivity structures are resolved by all three models, the differences between the models are significant.

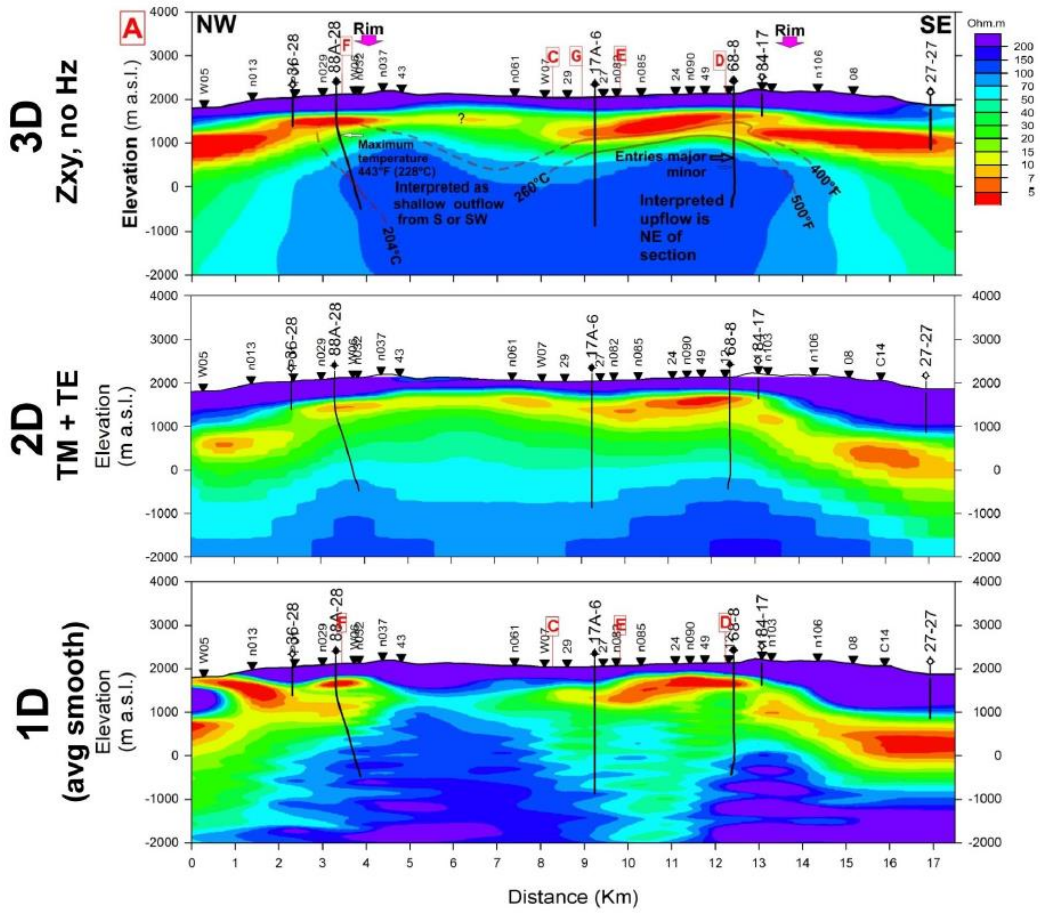

Figure 1 | Cross-section with 1-D, 2-D and 3-D resistivity inversions of the Glass Mountain geothermal field. Wells, isotherms and magnetotelluric stations are given. Note the differences in shape and depth of the conductive clay cap and resistive geothermal reservoir between the inversion. For details see (Cumming et al., 2010).

Distortion of the magnetotelluric signal and static shift

It is known that small near-surface conductive inhomogeneities and topography can cause distortion of the electromagnetic signal. Additionally, large scale regional structures, like the coastline, a large mountain range in the vicinity of the survey area or the dominant strike direction of geological structures, can cause a much less well understood distortion of the electromagnetic fields. All these distortions are commonly known as galvanic distortion.

A well-known example of galvanic distortion induced by amongst others near-surface inhomogeneities or topography, is the static shift effect (Sternberg et al., 1988). It's effect on the magnetotelluric data can be best described by a relative upward or downward shift in the amplitude of the apparent resistivity of the magnetotelluric transfer function from station to station, while the shape of the stations responses remains comparable (see Figure 2). As the static shift effect affects the resistivity model resulting from the measured magnetotelluric data, mitigation measures are necessary.

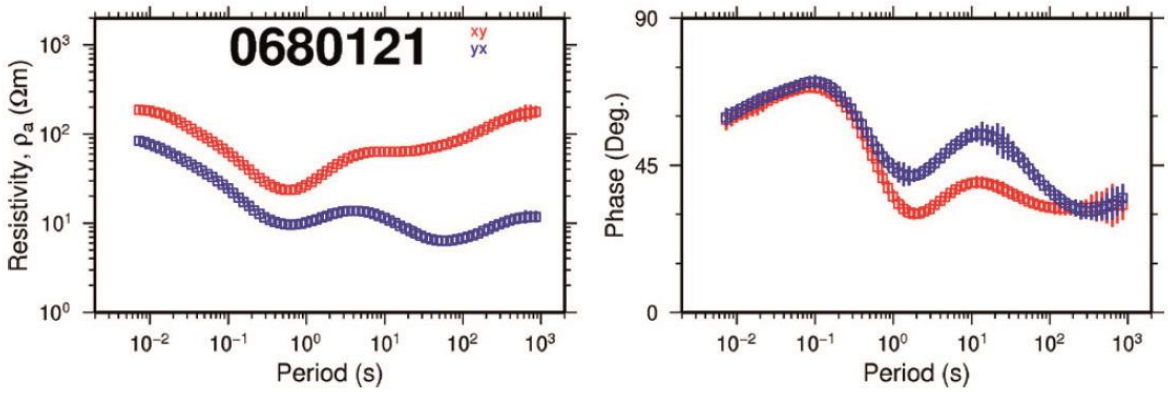

Figure 2 | Static shift effect in a magnetotelluric sounding. Here recognized in the large separation of the XY and Y X resistivity curves at periods below 1 s (Árnason et al., 2010).

Several approaches are available to correct for the static shift effect. (Árnason et al., 2010) for example, uses 1-D TEM measurements to iteratively shift the invariant of the magnetotelluric response towards the TEM response under the assumption that the TEM response reflects the true 1-D resistivity of the shallow subsurface. In other cases the magnetotelluric response is corrected by mapping the TEM apparent resistivity versus time to the magnetotelluric apparent resistivity versus period (Sternberg et al., 1988). Another approach is to correct for the static shift effect by smooth regularized joint inversion of the magnetotelluric data and static shifts. Ultimately, the last strategy to mitigate for the static shift effect is by incorporating the topography into the model mesh, under the condition of a sufficiently high resolution, and assuming that the 3-D inversion accommodates the correction.

Cultural electromagnetic noise

An electromagnetic measurement can also be distorted by man-made noise, often referred to as “cultural electromagnetic noise”. This electromagnetic noise can be caused by for example power lines, subsurface pumps, anti-corrosion systems in buried pipelines, wind turbines, electric trains, electric fences, and mining areas.

Cultural electromagnetic noise can be divided into passive and active electromagnetic noise. Besides these two types, a third type of cultural noise can be recognized, caused by for example passing vehicles or other artificial vibrations of the subsurface, this is often referred to as motional noise (Szarka, 1988). It is likely that in densely populated areas such as the Netherlands, the amplitudes of the electromagnetic cultural noise will be larger, sometimes exceeding the amplitude of the natural electromagnetic signal (Junge, 1996).

Passive noise sources such as roads, ditches, power lines, and pipelines, are redistributing the electromagnetic source field. Depending on the size of their local electromagnetic field, the influence of passive noise sources on the measurements can be avoided or minimized by placing the stations a considerable distance away. Some of these structures can also serve as an active noise source when inducing an electromagnetic (secondary) field into the subsurface. Examples of active noise sources are Direct Current (DC) railways, electric power transmission lines, subsurface pumping stations, and anti-corrosion systems in buried pipelines. Active noise will heavily disturb the measured electromagnetic spectra. When measuring far away enough from the noise source, its effect will be decreased.

As it is not always possible to avoid all sources of cultural electromagnetic noise during a magnetotelluric field survey, cultural electromagnetic and other noise effects must be eliminated from the magnetotelluric data during processing to obtain an accurate resistivity model of the subsurface.

Although still a significant factor, the influence of cultural electromagnetic noise on a CSEM measurement is reduced in comparison with a magnetotelluric measurement. By using a source signal the signal-to-noise ratio is improved.

Remote reference

To optimize the estimated electromagnetic transfer function the robust reference method is used in almost every magnetotelluric survey (Gamble, 1979). The remote reference method utilizes the plane wave assumption by simultaneously measuring the horizontal magnetic field at a remote station. Assuming uncorrelated magnetic noise between the local and the remote magnetotelluric station, the noise in the local station can be eliminated.

Electromagnetic data acquisition, processing and inversion

General EM workflow

In the following a generalized electromagnetic workflow is presented, a graphical version of the workflow is found in the Appendix. From start to finish:

1. **Survey preparations** comprise preparing the recording and transmitting equipment, locating station locations with respect to survey requirements, scope and EM noise sources. Organisation of the logistics of the survey including permitting and scouting of the selected locations. Selecting a location for the remote reference station when measuring MT and a location for the source dipole when conducting a CSEM survey.
2. Carry out the **survey**. Upon arrival at a station location, decide if the station location should be shifted (e.g. when a noise source is too close, or the slope too steep) and install the station. Check, and if necessary improve, the contact resistance of the electrodes. Finally, the acquisition parameters are set.
3. In case of an MT survey, the **data acquisition** is carried out during the night by the instruments. In case of an CSEM survey, the **data acquisition** is carried out in pre-defined time windows at a certain frequency.
4. The acquired time series are visually inspected during the first step of **data processing**. Following, they are transformed to the frequency domain. In the frequency domain, the data is processed using a variety of statistical tools after the which the transfer function is estimated, usually using a robust processing technique. Poor quality or physically implausible data points are removed from the processed data. Finally, a set of transfer functions per measured station becomes available.
5. To understand and explore the data, a **data assessment** is carried out by plotting the data at selected frequencies by apparent resistivity, phase, induction arrow, and/or polar diagram. Based on this assessment the dimensionality of the data is determined, transfer function rotated and 1-D inversions carried out.
6. Based on the 1-D model results, **maps at different depths** are created for apparent resistivity, phase, tipper, induction arrow and polar diagrams.
7. These maps form the basis to be able to **prepare EM inversion.** This includes rotation of the data, preparation of the model grid, including topography and bathymetry. Furthermore, geological knowledge and the 1-D model results help choose a set of initial models. Finally, a forward model is run to test the quality of the model grid and inversion parameters.
8. Carry out a **2-D or 3-D inversion** of the data.
9. Geological **interpretation of the resistivity model** results.

Magnetotelluric data acquisition

Station layout

Magnetotelluric surveys are conducted using data loggers measuring the five components, horizontal electric and full magnetic, of the electromagnetic fields. The horizontal electric field is measured using electrodes set up as two perpendicular dipoles, often orientated North-East and South-West. The non-polarizable electrodes are buried to account for day-night temperature variations in the upper few tens of centimetres of the subsurface. Magnetic coils measure the three components of the magnetic field. Two of the magnetic coils have their dipole positioned horizontally with a perpendicular orientation, measuring the horizontal magnetic fields, while a third magnetic coil is positioned vertical, measuring the vertical magnetic field. Since accurate and stable positioning of the coils is important, the coils are buried in shallow holes to prevent any external disturbances. The general layout of a

magnetotelluric station is shown in Figure 3. A GPS-receiver is connected to the data logger for time synchronization with the remote reference station. To power the data logger while measuring, a battery is also part of the setup of a magnetotelluric station.

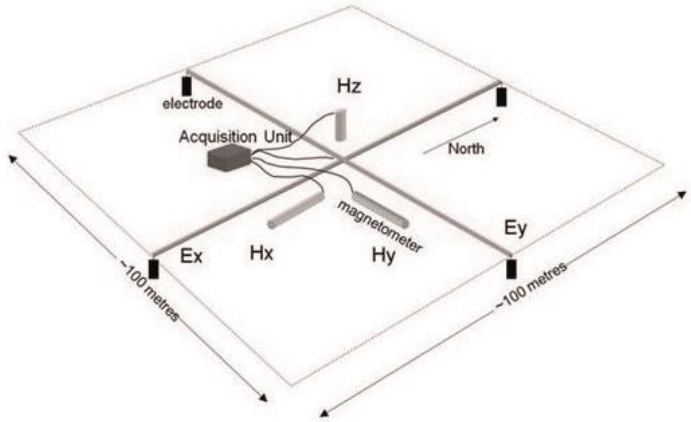

Figure 3 | Schematic MT station layout. Shown are the four electrodes measuring the two horizontal components (Ex and Ey) of the electric field and the three magnetic coils measuring the three components of the magnetic field (Hx, Hy, Hz). An acquisition unit (or data logger) is also shown, as are typical dimensions of a MT station.

Figure 4 | Images from MT equipment. From left to right, magnetic coil, electrode and a Phoenix MTU-A data logger with battery.

MT sounding period

Depending on the depth of the target of the magnetotelluric survey and the local bulk electrical resistivity of the Earth, the magnetotelluric sounding period varies from a few hours to several days, months or years. A possibility is to use the skin depth equation to estimate the desired magnetotelluric sounding period for a survey. A more sophisticated strategy is to determine the desired period range of the survey and adjust the magnetotelluric sounding period accordingly. The period T can be determined using:

$$T = \mu_0 \sigma \pi p^2.$$

Here σ is the bulk electrical conductivity of the subsurface in Sm^{-1}. To explore a geothermal reservoir from 0.5 to 5 km depth with an average bulk resistivity of 1 Ωm, a period $T = 1$ to 100 s is necessary. In practice the resistivity of the surface is not homogeneous and this simple computation becomes more complex. For geothermal exploration purposes it is common to record magnetotelluric data for roughly 18 to 24 hours. This sounding period

corresponds, depending on the bulk resistivity of the Earth, with penetration depths up to several kilometres.

Survey layout and preparation

The survey grid layout is determined by the local topography, size of the survey area, the available budget and time, and the expected dimensionality of the local geological structures. In geothermal exploration practice a few profile lines or a semi-regular grid layout with a site spacing of a half to two kilometres is the norm. The choice of the station spacing distance depends on the available time and budget as on the necessary detail of the resulting resistivity model. The MT survey layout for the exploration survey of the Montelago geothermal project is shown in Figure 5.

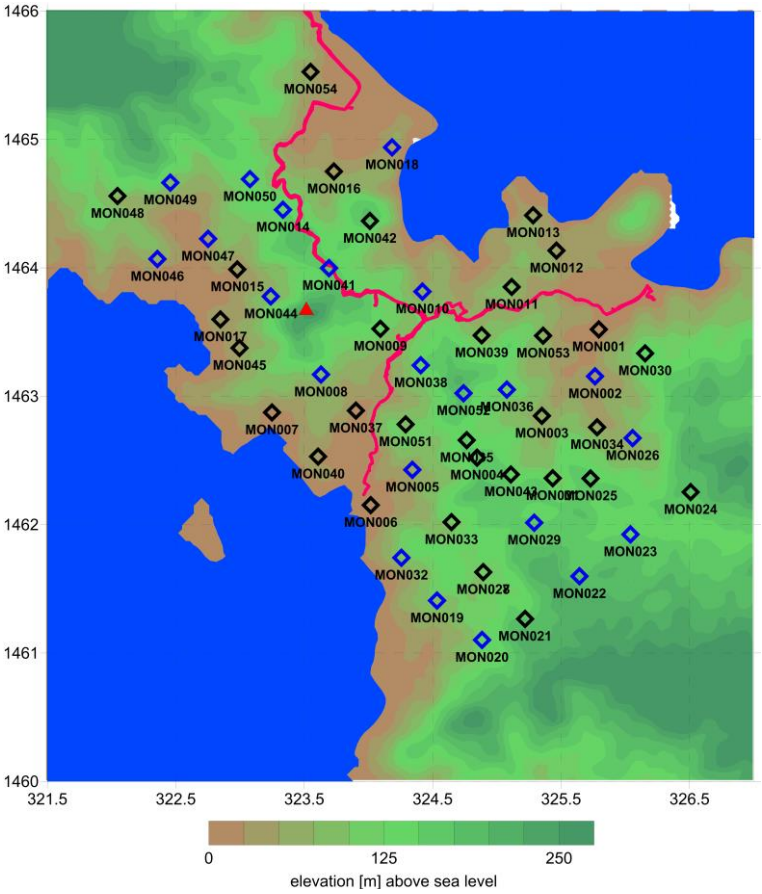

Figure 5 | MT survey layout for the Montelago Geothermal project. Shown are the elevation and the main roads (purple). The sea is located in the North-East, while in the South-West a lake is present. The red triangle represents the location of Mount Montelago, an ancient volcano. Full tensor MT stations are blue diamonds, and telluric (two components) MT stations are black diamonds (van Leeuwen et al., 2016).

During a magnetotelluric survey a remote station is often recording at an electromagnetically quiet location measuring simultaneously with the local magnetotelluric stations. Finding a good, quiet location for the remote reference station is always worth the effort for a successful magnetotelluric field campaign.

Another factor influencing the magnetotelluric data quality is the accuracy of the station layout in the field. The easiest way to acquire good data is to work accurately and assure that the field crew is working precisely. Regularly sites are set up too close to possible (cultural)

electromagnetic noise sources and with an inaccurate positioning of the coils or electrodes. Another straightforward mitigation procedure for distortion of the electrical field is ensuring good conductance between the electrodes and the Earth. Preparing strategies to tackle the possible difficulties of the terrain in the survey area and scouting the station locations prior to the field work or station occupation often increases the average data quality of the magnetotelluric survey. Finally, the strength of the magnetic field is influenced by the space weather. For the magnetic field this is forecasted and reported online as the Kp-index[2]. The higher the Kp-index at a location, the stronger the local magnetic field strength, and the more likely the acquired magnetotelluric data is of good quality. Consequently, if possible, a magnetotelluric survey should be carried out during a period of forecasted high Kp-indices. The altitude at which the magnetotelluric survey is conducted also influences the magnetic field strength.

A specific circumstance for the Netherlands influencing the survey layout of a magnetotelluric survey is the presence of a DC railway network. When a train passes, it acts as a moving electromagnetic source, disturbing the measured signal. Consequently, a station should be positioned far enough from the railway. As the Netherlands is a densely populated country, magnetotelluric stations should be positioned carefully. Ideally, a station is installed at a distance of a few hundred meter from potential electromagnetic noise sources. Also specific for the Netherlands is the publicly available data from hydrocarbon exploration. It is likely that the geographical location of this data will serve as a constraint when designing a magnetotelluric survey.

Crew, planning and costing

Due to very good accessibility, an MT survey in the Netherlands can be carried out with a relatively small crew. A two person crew driving a minivan can easily retrieve 3 to 4 stations and install 3 to 4 MT stations a day. Depending on the size of the survey, the available time and instruments, a survey can be carried out with one or several crews. For larger surveys, when working with at least three field crews, a chief geophysicist and data processor stationed at the base camp are required.

A good MT survey starts with a scouting expedition which has two goals. First, to secure access to the planned station locations from the land owners. Second, to check if there are EM noise sources nearby and if the planned station should be relocated.

When the crew and the instruments reach the survey base camp, the first two days are spend on the preparation, testing and calibration of the instruments and receivers as well as on installing and testing the quality of the remote reference station. As MT stations measure their signal during the night, during the day stations are retrieved, moved to a new location, and installed again. After the survey is finished, another day is used to clean and pack the instruments.

[2] https://spawx.nwra.com/spawx/env_latest.html and https://www.swpc.noaa.gov/products/27-day-outlook-107-cm-radio-flux-and-geomagnetic-indices

Following this basic schedule, a survey crew consisting of 3 field crews and equipped with 12 full stations, can run a 60 station survey in approximately 9 days.

- 2 days preparation and calibration of instruments in installing the remote reference stations;
- 1 day installing 12 full tensor MT stations;
- 4 days retrieving and installing 12 stations a day;
- 1 day retrieving 12 stations and start cleaning of instruments.
- 1 day cleaning and packing of instruments.

Theoretically, this crew can produce at rate of 12 stations a day, in practice, due to technical and other issues, stations must be re-acquired, daily production will be lower, and the survey time longer.

Two cost models exist for MT surveys. The first model is that instruments and staff are hired at day rate. The second model is based on a fixed price per station, in this model there is often an arrangement about the percentage of the stations that should be technically sound. This second model is more common in the geothermal world. Both models have a separate mob/demob price. In Table 1 a price range for a 60 station survey is given.

Table 1 | Per station budget estimate for a 60 station survey. Included in the per station price are besides the MT data, also in field QAQC, data processing and reporting. Pre-survey scouting and permitting is excluded in this budget estimate.

Item	Unit	Price (€)	Budget estimate (€)
Pre-survey modelling	1	5.000 - 8.000	5.000 - 8.000
Mob/Demob	1	5.000 - 10.000	5.000 - 10.000
Price per station	60	750 - 1.250	45.000 - 75.000
Total			**55.000 - 93.000**

Inversion modelling is often budgeted separately, sometimes using fixed price based on a hours times budget model or again using a price per station. For the 60 station example discussed here, a 3-D inversion will take approximately 4 weeks, so 20.000€ lump sum or 333€/station.

Controlled-source electromagnetics

Transmitter and receiver layout

A CSEM survey consists of one or several transmitter electric-field dipoles of approximately 1 km long. This length is long enough to get sufficient power into the ground and small enough to have sufficient resolution (Schaller, 2018). Using, a T-shaped geometry allows for un uniform azimuthal distribution of the injected source field. As shown in the photo in Figure 7, metal stakes are used to ground the dipole. The dipole is connected to a transmitter which is powered with a generator. The transmitter feeds an high-power, high-voltage signal generator. The signal generator feeds the current into the electrodes. A schematic diagram of the CSEM source is shown in Figure 6.

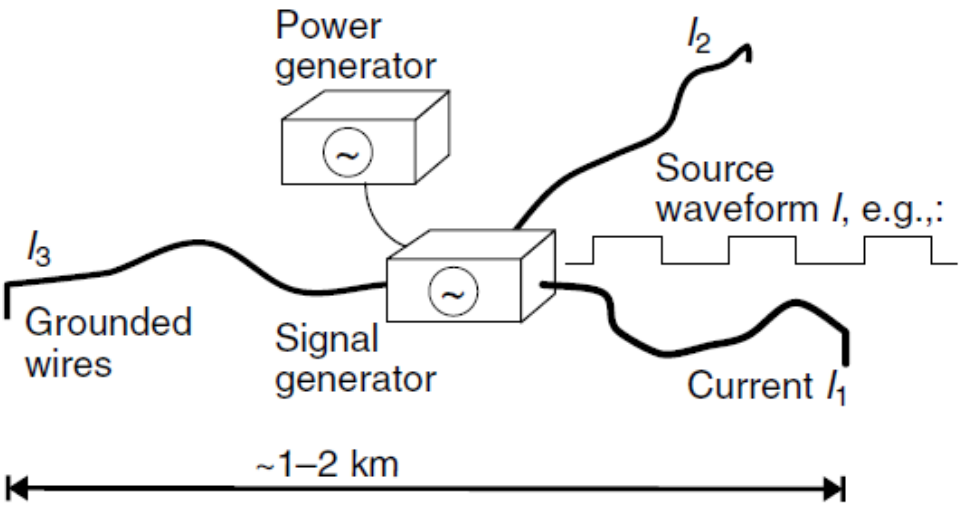

Figure 6 | Schematic diagram of a CSEM source. Shown are three grounded wires via which current is injected into the ground, the power generator and the signal generator. Dimensions of the source are also given, as is the shape of the source waveform (Streich et al., 2013).

Figure 7 | Images from CSEM components. From left to right: installed data logger for a telluric CSEM station (only E-field). The orange cables are connected to four electrodes orientated in a square. One injection point of a CSEM source consists of a few metal stakes connected to a wire, to ensure good conductivity with the subsurface, brine water is used.

The setup of the source-receiver configuration is dependent on expected subsurface properties and scope of the survey. In Figure 8, a set of the responses of a different source-receiver combinations is shown for two different background models. Where a conductor in a resistive background model is detected by all source-receiver combinations, only in the cases of a x-directed horizontal dipole source with an E_x or E_z oriented receiver is able to detect a resistor in a conductive background. This last subsurface resistivity distribution is what we expect to find in the Dutch subsurface.

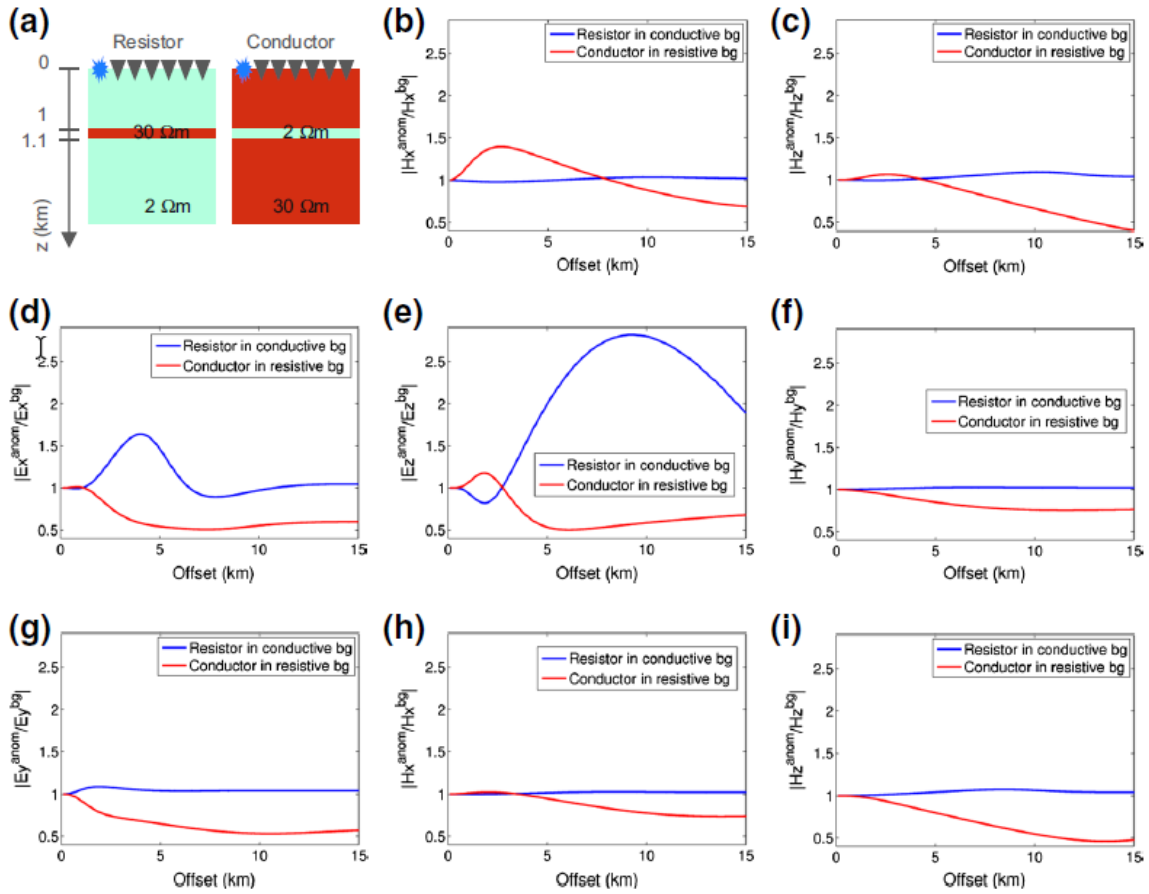

Figure 8 | Modelled station responses dependent on the source configuration. Blue lines show the station responses of a resistor in a conductive background (left model in a) and red lines show the station responses of a conductor in a resistive background (right model in a). b) vertical magnetic dipole (VMD) source and field component Hx, c) VMD and Hz, d) x-directed horizontal dipole (HED) and inline Ex, e) x-directed HED and Ez, f) x-directed HED and Hy, g) y-directed HED and Ey, h) y-directed HED and Hx, I y-directed HED and Hz (from Streich, 2015).

Similar to an MT setup, CSEM receivers, as shown in Figure 7, generally record the five components of the electromagnetic field, consisting of the horizontal electric field and the three components of the magnetic field. In some cases, the three components of the electric field are measured. The non-polarizable electrodes are used to measure the electric. The magnetic field is measured using magnetic induction coils. The electrodes and magnetic coils are connected to a receiver unit.

As the magnetic field is laterally relatively smooth, in CSEM practice, the survey layout often consists of a clever mix of receiver stations only measuring (the variations in) the electric field and receiver stations measuring both (the variations in) the magnetic and electric fields.

Survey layout and preparation

Depending on the target of the survey, the distance between the source and receiver stations is roughly 2 to 5 km. At shorter distances, receiver stations measure a complex near-source signal which hardly contains subsurface information. At longer distances, the signal-to-noise

ratio of the recorded signal is too low. The size of the survey area determines if one or several CSEM source locations are necessary.
To achieve an uniform azimuthal distribution of the CSEM source fields, three transmitter electrodes should be arranged in an equilateral triangle with the generator in the center and injecting source currents at multiple polarizations (Streich et al., 2013). In practice, this is not necessary or possible due to practical field constraints, and L- or T-shaped source geometries are used.

Similar to a MT survey, receiver stations can be aligned in arrays, for 2-D coverage, or in a grid, for 3D coverage. The spacing between the receiver stations determines the lateral resolution of the measured data.

Recording time

High injection frequencies resolve structures with high resolution and shallow depths, while low injection frequencies penetrate to greater depth with a lower resolution. Depending on the depth and characteristics of the target, a modelling study guides determining the injection frequencies and optimal receiver – transmitter distance (see Figure 9). The number of and the values of the injection frequencies determine the total injection time at a transmitter location during a survey. Higher frequencies require shorter injection times, while lower frequencies require longer injection times.

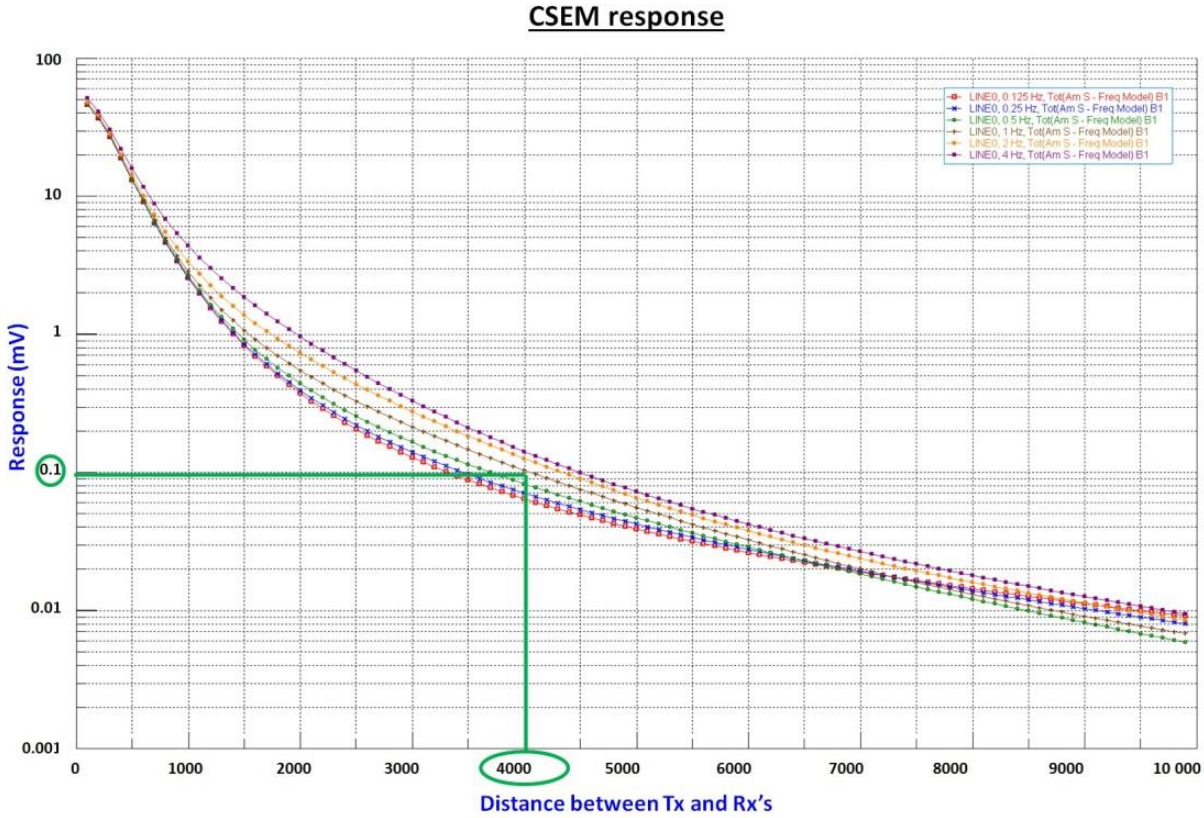

Figure 9 | Modelled signal respons at a CSEM receiver station (vertical axis) versus the distance between receiver (Rx) and transmitter (Tx) using a transmitter dipole of 1 km and targeting a reservoir at roughly 2 km deep. In this case a 0.1mV response is acceptable and a maximum distance between Tx and Rx of 4 km is allowed using injection frequencies of 1 Hz and higher.

Crew, planning and costing

Although the installation of dipole and the transmission of electrical current into the ground is involved, the costs for a CSEM survey, or combined MT-CSEM survey, are comparable to an MT survey. Besides the extra instrumentation for the source, for the transmission of the source signal an extra crew member is necessary, this must be someone with the right qualifications to operate a high voltage instrument. Furthermore, as for a CSEM survey the magnetic field is not measured at every station, a two person crew can install 6 to 8 CSEM stations per day.

As CSEM involves the transmission of a source signal, it is best practice to first install all CSEM stations and then inject the source signal. To ensure good signal to noise ratio at all stations, several sweeps from different injection dipole locations are often carried out when a larger area is surveyed. When research area becomes too large for this strategy, a sequence of sweeps over different subareas will be a good data acquisition strategy. As it often takes several days before the entire survey area is covered by CSEM stations, the full EM tensor stations can be set up such that they measure MT signal during the night.

Similar to an MT survey, for a CSEM fieldwork a scouting and permitting expedition should be carried out prior to the actual survey.

Again, carrying out a hypothetical survey of 60 CSEM stations will take approximately 11 days. Of this survey every fifth station is a full tensor EM station. This can be achieved when the survey is planned following the schedule below:

- Two days unpacking, preparing and calibration of instruments, installation of remote reference.
- Five days to install 60 CSEM stations with two CSEM crews of two persons and one MT crew with two persons. Preparation of two injection dipoles
- One day for the transmission of source signal from two locations.
- Two days retrieval, cleaning and packing of instruments.

Quick data processing for QAQC is carried out in the field, while the final processed data and field acquisition report is generally delivered about one month after the last survey day.

A CSEM survey is commonly budgeted using the same cost models as for MT surveys. Although extra personnel and additional instruments are required, for a similar number of stations, a similar budget estimate is expected (see Table 1). This can be explained by the fact that the number of stations recorded per day of a CSEM-MT survey is higher when compared to an MT survey. Consequently, less staff per station is necessary for a CSEM-MT survey. Like with MT data, the CSEM modelling is often budgeted separately.

Combination with seismic data acquisition

An MT, CSEM or combined MT-CSEM survey can be carried out simultaneously to a seismic survey. As the impact on the environment, logistic complexity, number of instruments, and permitting procedures of these surveys on the environment are significantly smaller in comparison to a seismic campaign, running a EM campaign in parallel to a seismic campaign should be relative easy to organize. An advantage of running a simultaneous survey is that the EM campaign can benefit from the logistic and permitting efforts carried out for the seismic campaign. Additionally, as processing and interpretation take time, a parallel survey open the opportunity to build an integrated subsurface model based on both EM and seismic data simultaneously.

Processing and inversion of electromagnetic data

In Figure 10 a generalized workflow of electromagnetic data processing and inversion is presented. In the paragraphs to follow details of each steps are discussed. The first steps in EM data processing consist of the data handling and preparation of the recorded time series (TS), finalized by transformation to the frequency domain into Fourier coefficients (FC). Using these Fourier coefficients (FC), transfer function (TF) estimates are computed using robust regressions techniques. The created transfer function estimates are analysed and if necessary edited, after which they are prepared for inversion (INV). Other steps in the inversion process are grid design, testing the inversion strategy and the inversion modelling itself.

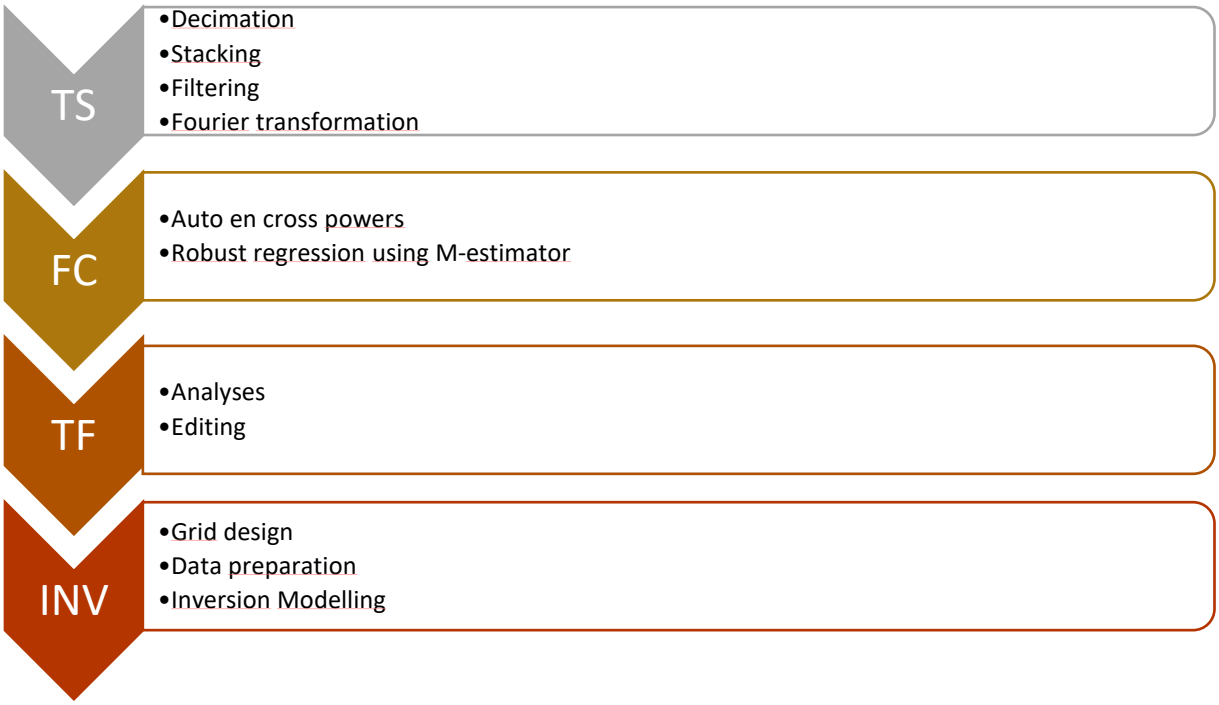

Figure 10 | Generalized workflow of electromagnetic data processing and inversion showing the main steps in the process. TS = timeseries data, FC = Fourier coefficients, TF = transfer functions, INV = inversion.

Processing of electromagnetic data

At this point it is necessary to mention that in electromagnetic data processing the raw time-dependent data (TS in Figure 10) is transformed to the frequency domain (FC in Figure 10). To fully utilize all measured frequencies in magnetotelluric or controlled-source electromagnetic station, the time-series (TS) are decimated, creating a number of time-dependent data sets with decreasing sampling rates. Depending on the sampling rate and the number of samples present, each decimation level spans a number of frequencies. Following, the individual samples are stacked along pre-defined overlapping time-windows. The data is smoothed by applying for example by a running average filter to the stacked time windows. Finally, the stacked time-windows are transformed to the frequency domain using a direct or fast Fourier transform to estimate Fourier coefficients (FC in Figure 10).

To recover the resistivity of the subsurface in the spectral domain the transfer function, has to be estimated. As is often the case of actual electromagnetic measurements, the recorded electrical and magnetic fields contain noise and not only the transfer function but also its uncertainty has to be estimated. The transfer functions (TF in Figure 10) introduced before can in the spectral domain be generalized using the expression:

$$X = Z_1 \cdot Y_1 + Z_2 \cdot Y_2,$$

where X is the predicted channel associated with either E, H, or B_z and Y_1 and Y_2 being the predicting channels B_x, B_y or I. Z_1 and Z_2 are the transfer functions of a linear system of equations, e.g. Z_{xx} and Z_{xy} or $T_{1,3}$ and ${T_{1,3}}^{E_x}$ and ${T_{2,3}}^{E_x}$. The magnetotelluric transfer function can be estimated by robustly weighted least-squares fitting (Chave et al., 1987; Chave and Thomson, 2004; Egbert and Booker, 1986; Larsen et al., 1996). These approaches utilize unbiased statistical estimators and data adaptive weighting-schemes for the calculation of the magnetotelluric transfer function.

As solving this system of equations using the least-squares principle often delivers unreliable results when applied to real electromagnetic data, it is hardly used in practice (Chave and Jones, 2012). Robust processing approaches are used instead to estimate the electromagnetic transfer function. In robust processing approaches the norm of the errors in $X = (Z_1 \cdot Y_1 + Z_2 \cdot Y_2) + \varepsilon$ is minimized without letting the extreme outliers dominate the result.

Inversion of electromagnetic data

To estimate the subsurface resistivity distribution in the Earth's subsurface, the observed electromagnetic data needs to be inverted. The process of inversion is iterative and is aimed at finding one or more resistivity models whose predicted response matches the observed data as good as possible. Depending on the properties of the station response and the dimensionality of the local geology the inversion can be done in 1-D, 2-D or 3-D. The resulting inversion model is non-unique, i.e. the responses of several resistivity models fit the observed electromagnetic data equally well. Consequently the inversion of electromagnetic data is inherently unstable, or ill-posed, and the solution estimated must be constrained using other sources of information.

The inverse problem can be formulated as:

$$d = F(m) + e,$$

where d is the data space, a vector containing the observed data, e.g. the electromagnetic transfer function, the apparent resistivity and phase, or the conductivity. The vector e contains the data errors of d. The model space m represents the real resistivity values of the Earth, while F is a forward function predicting the theoretical values of the data for a hypothetical (model) representation of the Earth. In the theoretical case $e = 0$, the solution becomes $m = F^{-1}(d)$, hence the term inverse problem.

The basis for much geophysical inverse theory is the least-squares estimation. A least-squared solution is defined as finding the minimum solution of a fitting function, estimating the goodness of the fit between the model and the observed data. This data misfit can be expressed by a penalty function

$$\Phi(m) = \big(d - F(m)\big)^T \bar{W}(d - F(m)),$$

where $\bar{W}$ is the weight matrix containing pre-assigned weights (Egbert and Kelbert, 2012; Siripunvaraporn, 2012), and $r = d - F(m)$ is the residual vector. Minimizing $\Phi(m)$ is done by starting from some initial model and iteratively solving the inverse problem until a predefined data misfit is reached.

Electromagnetics in geothermal exploration abroad

Electromagnetic methods and especially the magnetotelluric method is generally deployed in the exploration phase of high enthalpy or volcanic geothermal projects. The reason for this is that the resistivity signature of a high enthalpy geothermal reservoir is a low resistivity layer overlying a more resistive geothermal reservoir structure. This is an effect of the geothermal fluids alterating the clay mineralogy forming clay minerals with a distinct range of resistivity values. This phenomena is well described by Flovenz et al. (2005). As geothermal fluids are related to volcanic activity, clay alteration is not expected in the Netherlands. Other factors, besides the resistivity of the rock, which influence the resistivity of a formation are the temperature, formation water composition, and the porosity and the permeability (van Leeuwen, 2016). The clay alteration mineralogy is in high enthalpy geothermal often used to predict the temperature of the fluids in the geothermal reservoir. The relation between temperature and clay alteration minerals is shown in Figure 11.

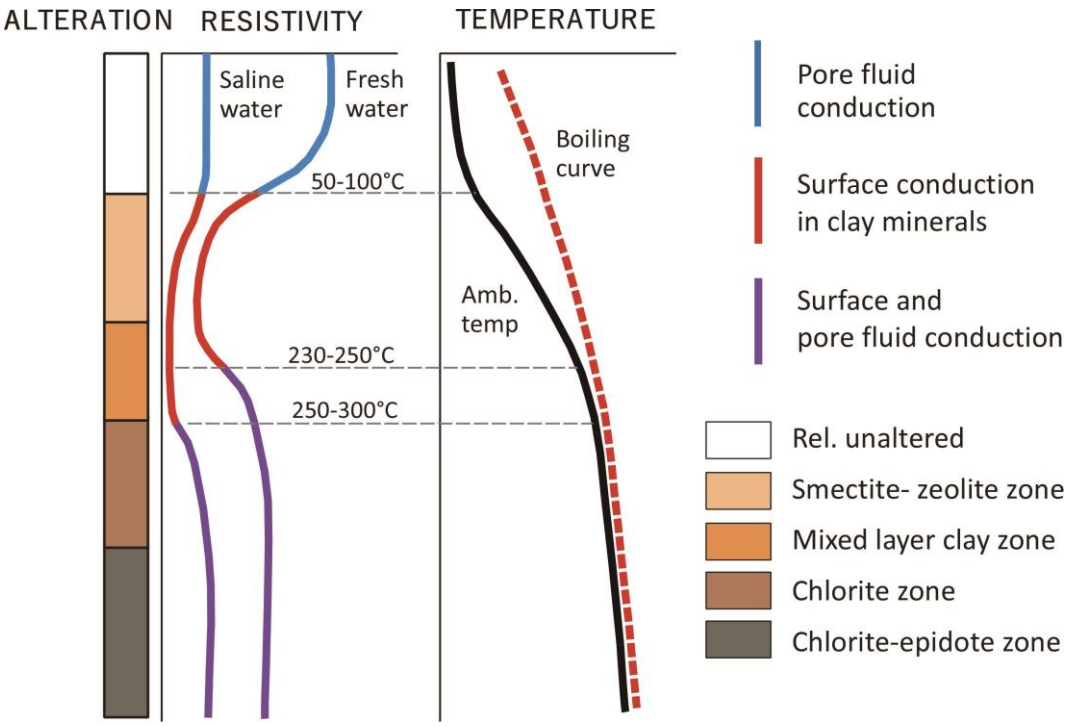

Figure 11 | Generalized resistivity structure of a basaltic geothermal system. From (Flovenz et al., 2005). Plotted as a function of depth are from left to right, the clay alteration, the electrical resistivity of saline and fresh water and the ambient and boiling temperatures. In the resistivity curves, the type of conduction, either pore fluid or mineral, is indicated. At temperatures up to 70 °C these minerals are smectite and zeolites having a high electrical conductivity. At temperatures between 180 °C and 220-240 °C a mixture of these clay minerals with illite, in acidic regimes, and/or chlorite, in basaltic regimes, are found. These newly formed clay alteration minerals tend to reduce the conductivity. Above 240 °C the smectite and illite have completely disappeared and a pure cholorite or illite zone is formed and bulk conductivity is increasing again. At even higher temperatures epidote is added to the alteration mineralogy.

To demonstrate the applicability of electromagnetic methods as a geothermal exploration tool, a selection of case studies is presented below.

The Krýsuvik high temperature geothermal area

The Krýsuvik high temperature geothermal area is located in southwest Iceland on the Reykjanes Penisula. It located in one of the northeast-southwest trending volcanic systems present on the peninsula. The Svartsengi and Reykjanes geothermal fields in the area have a combined installed capacity of 175 MW_e, while the Svartsengi field is also providing 150 MW_{th} for domestic heating (Hersir et al., 2018).

The data on which the 3-D resistivity model is based consists of 102 MT soundings irregularly placed in a grid with station distances from 5 to 10 km. After acquisition the data was processed and static shift corrected after which a 3-D inversion was carried out to construct a 3-D resistivity model. The Krýsuvik geothermal field is a perfect example of a geothermal resistivity structure of a conductive cap of alteration clay minerals overlying a resistive core (Flovenz et al., 2005; Pellerin et al., 1996) as shown in Figure 12. The deep seated conductive body at around 2 km depth is probably connected to the heat source of the geothermal field in the form of the emission of gas or dehydration (Hersir et al., 2018).

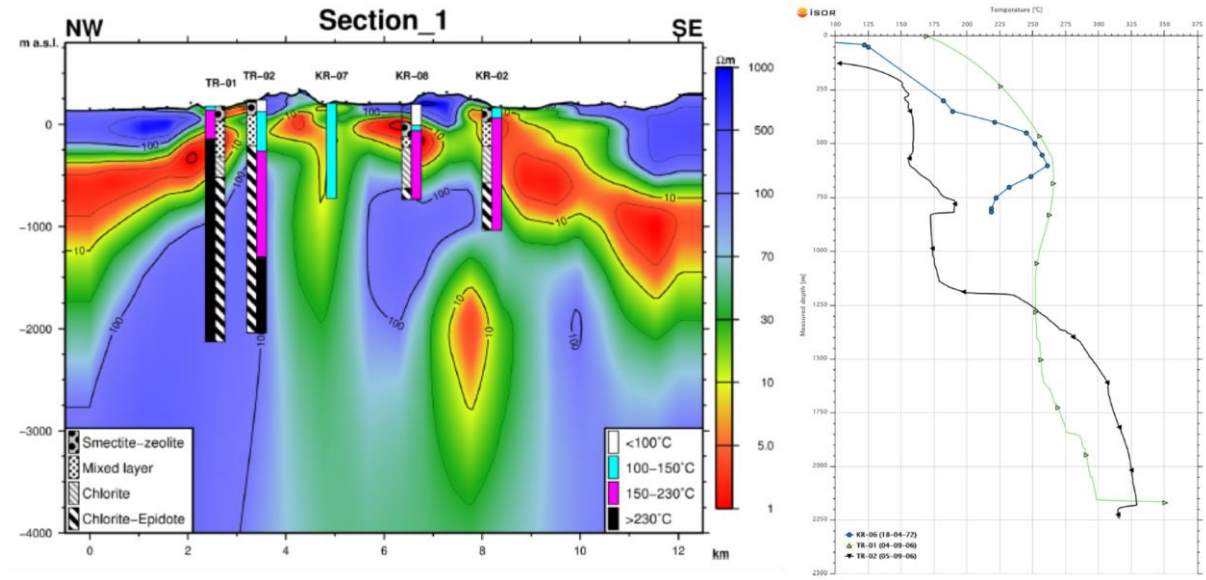

Figure 12 | Left panel: NW-SE striking resistivity cross section from a 3D resistivity model of the Krysuvik geothermal area. Clearly visible are the conductive clay cap and the resistive core. The resistive material on top of the clay cap consists of cold and unaltered rocks. Also indicated are a series of deep and shallow boreholes, included temperatures and clay minerology. The temperature measurements of the two deep wells are shown in the right panel. Right panel: temperature measurements in the boreholes KR-06 (not on the cross section) and the two deep wells TR-01 and TR-02. A temperature inversion is observed at shallow depth, while deep drilling revealed a resource of over 300 °C. Modified from Hersir et al. (2018).

The Gediz Graben geothermal area

One of the largest extensional graben systems in Western Anatolia in Turkey is the Gediz Graben. The geothermal area discussed here is located in the eastern part of the Gediz Graben. The lithology of the area consists of a basement of metamorphic rocks with a moderate resistivity and the sedimentary deposits covering the basement are divided into three main layers. At the base there is a relatively conductive conglomerate/limestone unit. This unit is overlain by a sandstone/claystone unit with high conductivities as a result of geothermal alteration. In fact, seismic data shows that this unit can be divided into two

separate layers. As there is no resistivity contrast between the two layers, the unit is considered as a single layer. Above the sandstone/claystone unit alluvial deposits are found, these deposits have a moderately high resistivity. The main reservoir in the area is the basement unit which has a highly variable porosity and permeability. Being highly fractured, the limestone rocks in the area have good reservoir properties as well (Erdogan and Candansayar, 2017).

The aim of the study presented here is to identify drilling targets for geothermal production based on a resistivity model of the Gediz Graben. To be able to model a realistic resistivity structure of the graben, information from 13 2-D seismic lines and data from 18 boreholes was used to construct a 3-D synthetic forward resistivity model of the entire area. For an area located north in the graben, a commercial MT data set was 3-D inverted using the strategy developed to construct the synthetic forward model. Based on the resistivity model of which is cross section is presented in Figure 13, production and injection boreholes were planned and successfully drilled, all boreholes were targeting faults related to resistivity anomalies. The graben geometry is clearly visible in the cross section, including two steep faults. The resistivities of the formations align with the lithologies found in the boreholes. Two deep production wells and one shallow injection well including their lithology are projected on the resistivity cross section. The production wells PW1 and PW2 are currently producing 350 m3/hr and 400 m3/hr respectively (Erdogan and Candansayar, 2017).

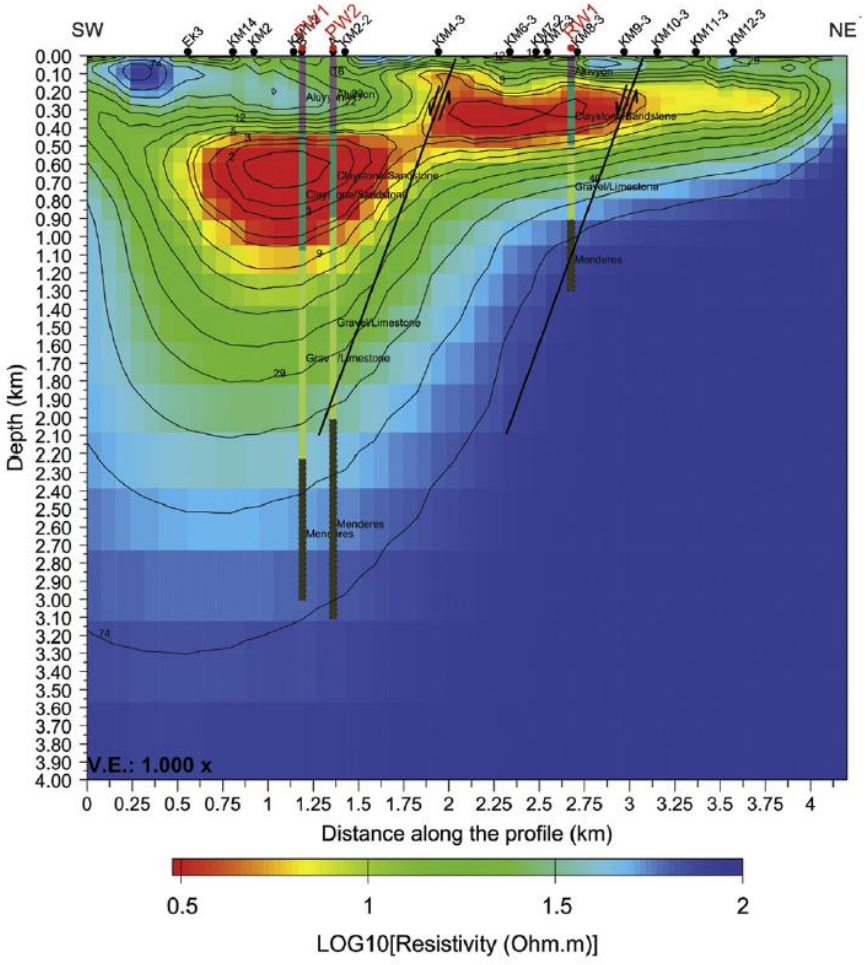

Figure 13 | Resistivity cross section extracted from the 3D inversion model of the MT data. From (Erdogan and Candansayar, 2017).

In this case study 2-D seismic data was only used to guide the inversion strategy and initial model parameters of the electromagnetic data into a 3-D resistivity model of the subsurface. Utilizing the interpretation of 3-D resistivity model, drilling targets for geothermal production were identified.

Geothermal potential of the Rathlin Basin, Northern Ireland

The Rathlin Basin in Northern Ireland is a sedimentary depocenter with reservoirs comprising hydrocarbons and an elevated geothermal gradient. This case study is presented as it bears several similarities with the conditions in the Netherlands; a sedimentary basin with hydrocarbons and several sources of EM noise. Although several geophysical data sets are available, the onshore portion of the basin has been surveyed with the MT method to evaluate the geothermal potential of the basin (Delhaye et al., 2019).

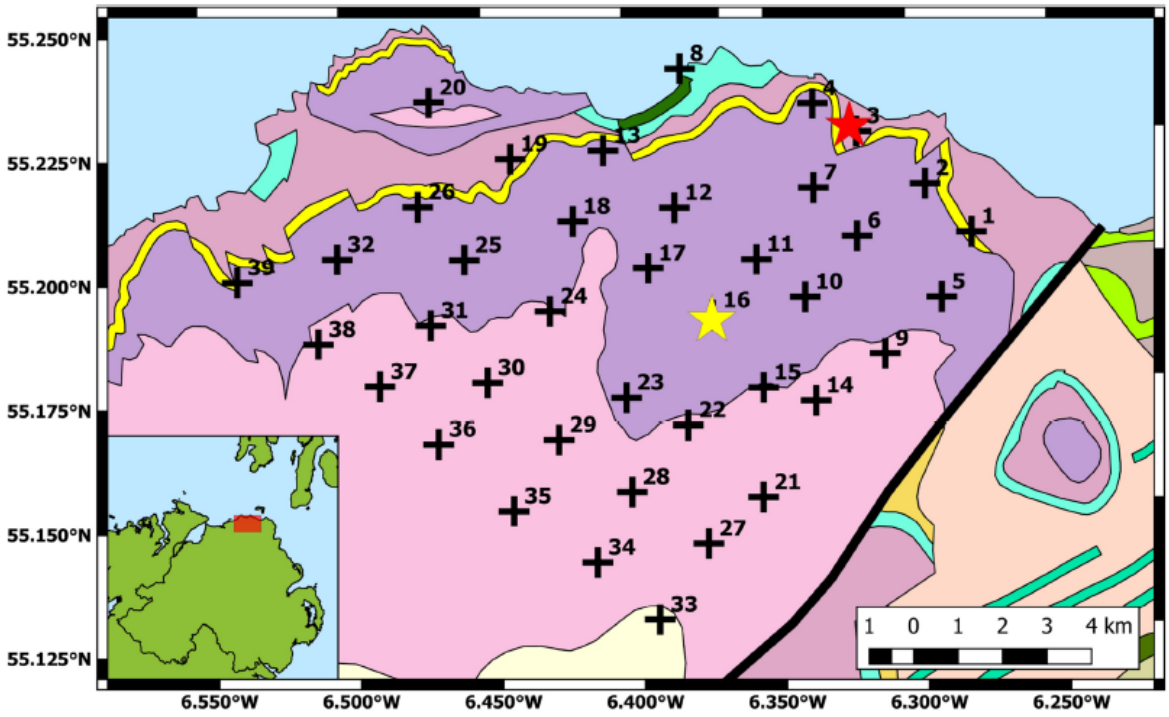

Figure 14 | Surface geology of the Rathlin Basin, Northern Ireland. The main units are in purple the Causeway Tholeiite and in pink the Upper Basalt Formation. The distinct yellow band is a interbasaltic formation of laterite/bauxite, north of this band lies the Lower Basalt Formation. A major fault in the east is shown as a bold black line. The black crosses represent MT stations and the two stars are the boreholes PM1 (red) and B1 (yellow) For details see (Delhaye et al., 2019)).

A series of 1-D resistivity models was made based on the acquired MT data and compared to the resistivity logs measured in the two boreholes. Figure 15 shows the model adjacent to the PM1 borehole. Since correlation the geological formation to the resistivity model was difficult, a statistical approach was used, resulting is as series of resistivity models of which the various statistical properties are presented (mode, median, mean, 10^{th} and 90^{th} percentile). The top of the reservoir formation of Permian age is not clearly resolved by the model. In general, the model is consistent with the formations drilled in the borehole, with the exception from a shallow dolerite formation.

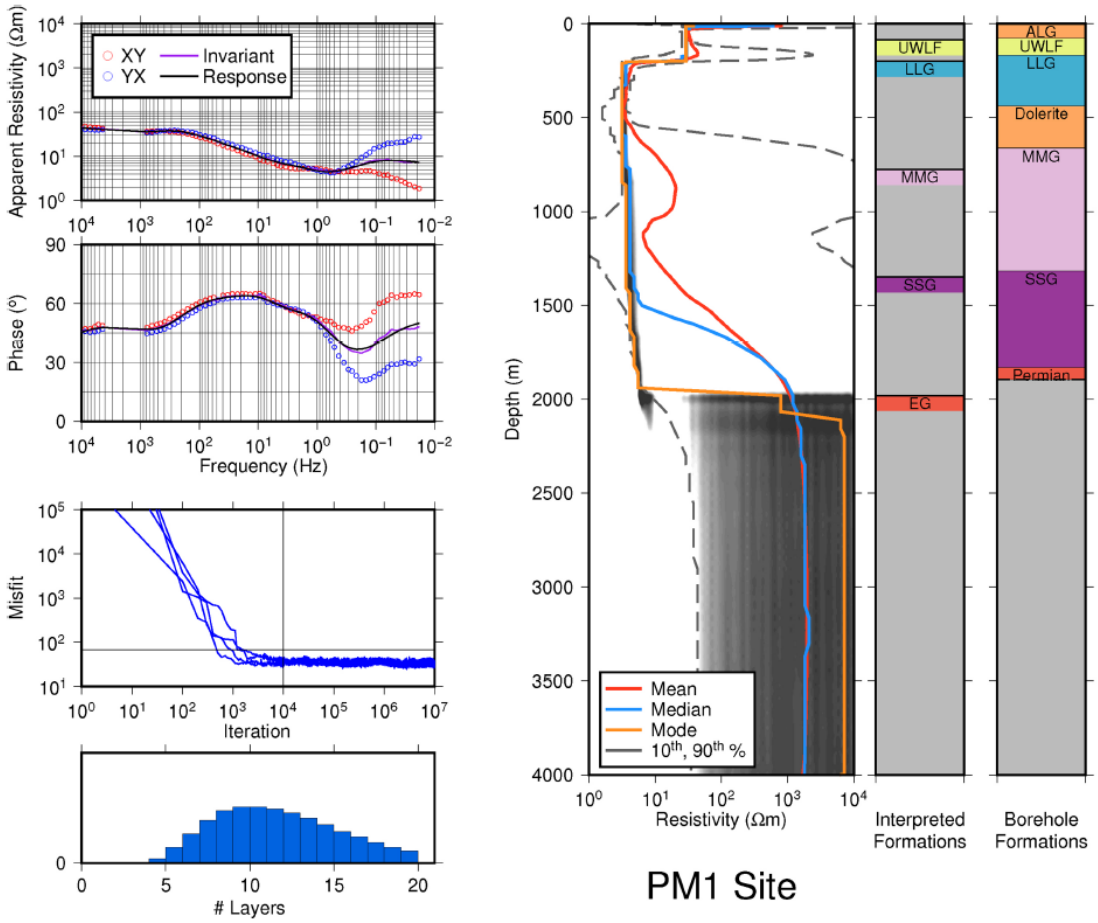

Figure 15 | Left hand side upper to panels show the MT station response of the station adjacent to borehole PM1. The lower two panels show statistics from the inversion model. The right hand side shows the 1-D resistivity model, interpreted and borehole formations. The shaded heatmap represents the normalized model probability density. UWLF is an Early Cretaceous limestone formation, LLG is an Early Jurassic mudstone formation, MMG is Late Triassic mudstone formation, SSG is an Early Triassic sandstone formation, and EG is an Early Permian sandstone formation. See (Delhaye et al., 2019) for details.

In this case it is demonstrated by means of MT data a 3-D model resolving the geological formations layers in a sedimentary basin can be constructed, adding in depth understanding to the available subsurface data. An important conclusion from this study that accurate resistivity values of the targeted sandstone layer – which is situated below a claystone layer – cannot be determined due to the resistivity configuration of the subsurface.

Electromagnetics in the Netherlands

Previous experiences with magnetotellurics and controlled-source electromagnetics in the Netherlands

The CSAMT experiment to image the Broek salt dome

A CSAMT experiment was conducted in 1998 to image shallows salt structures in the north of the Netherlands (den Boer et al., 2000). Mainly due to the large resistivity contrast between the salt, which is very resistive, and the overlying sediments, which are conductive, top of the salt was successfully resolved. CSAMT stands for controlled-source audio-frequency magnetotellurics. Additional time-domain electromagnetic (TDEM) measurements were carried out to correct for the static shift effect in the CSAMT data.

Like MT, AMT measures the natural time-variations in the Earth's electromagnetic field, only at higher frequencies. When using a source in combination with AMT, and thus maintain the plain wave assumption, the source must be located far away enough from the receivers. In contrast to a CSEM source, a CSAMT source injects current over a range of frequencies. This approach delivers data corresponding compatible with MT data processing methods.

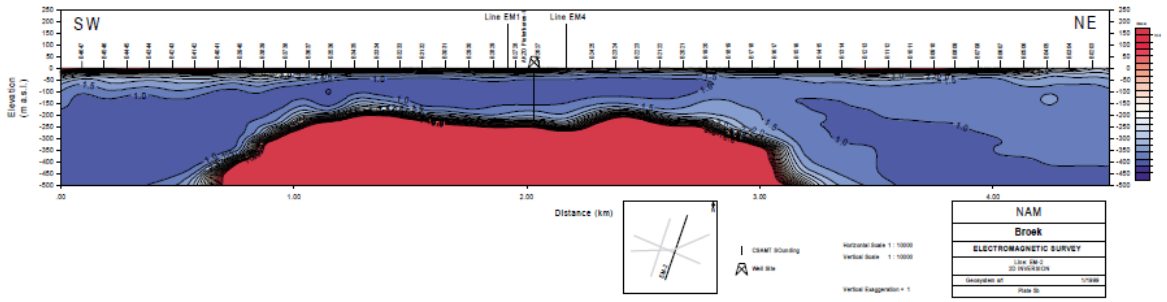

Figure 16 | Roughly North-South oriented 2D resistivity model from the Ommelanderwijk CSAMT survey. The outline of the salt dome is clearly visible (from (den Boer et al., 2000).

Using the resistivity models from the CSAMT survey, of which an example is shown in Figure 16, a new Pre-SDM processing of the seismic data was carried out. The interpretation of this seismic volume resulted in much better imaging of the salt body and sub salt structures as shown in figure 17.

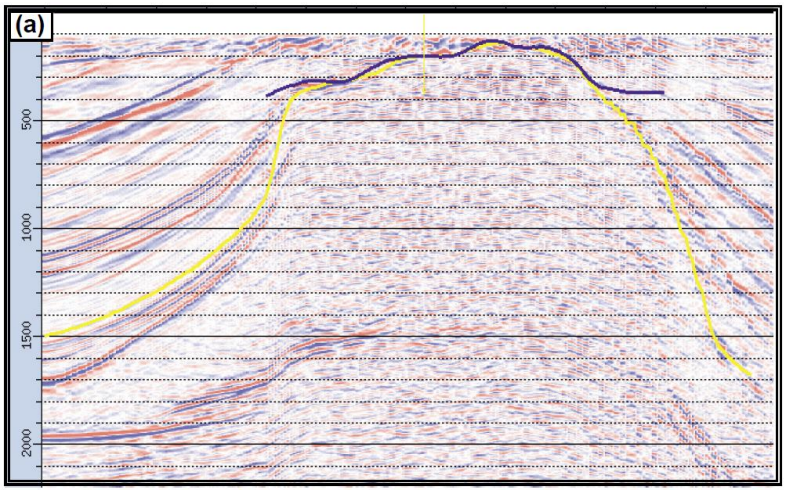

Figure 17 | EM result improved seismic interpretation of a salt dome (from den Boer et al., 2000)

MT pilot at the Drents-Friese Wold

A two station MT pilot was conducted in the Drents-Friese Wold area with a remote reference station at the island of Texel in 2012. Important lessons were learned with respect to acquiring MT data in the Netherlands, but due to local EM noise source, no good quality MT data was acquired.

To ensure no influence from passing trains, the pilot location was chosen at a distance of a least 10 km away from an electrified railway. Based on this map a location in the north of the Netherlands was selected. During the pilot, no train noise was measured. However, other EM noise sources were detected. As illustrated in Figure 18, this was an EM signal generated by an electrical fence (right panel) and another distinct EM noise source, probably caused by (drainage) pumps (left panel).

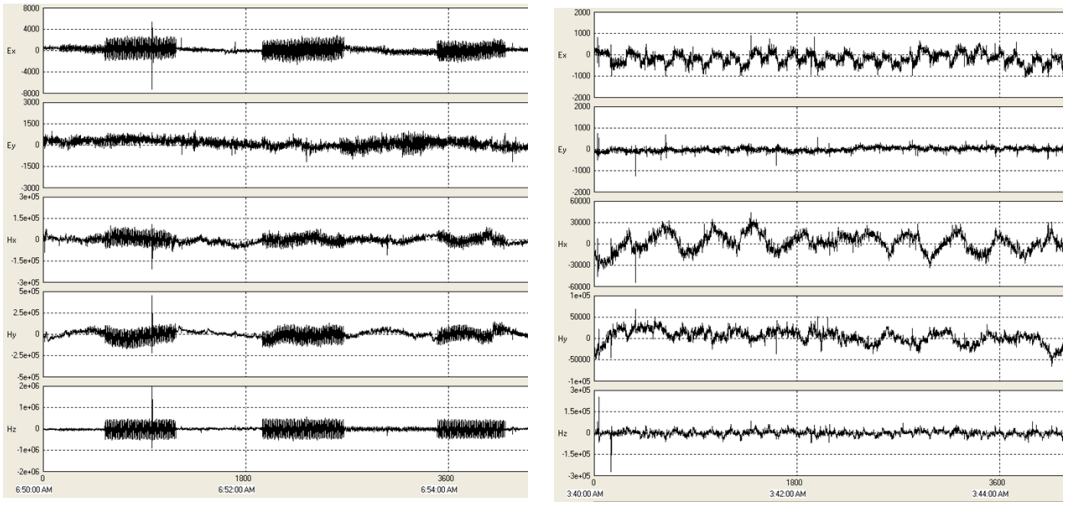

Figure 18 | Time series of EM noise measured during the MT pilot. From top to bottom: Electric Ex signal, electric Ey signal, magnetic Hx signal, magnetic Hy signal and magnetic Hz signal. Left panel: signal from pumps. Right panel: signal from electric fence.

Two CSEM – MT experiments related to geothermal in Belgium

Since 2015 two combined CSEM and MT experiments were carried out in Belgium. The first experiment from September 2015 is related to the Balmatt geothermal project near Mol (Coppo et al., 2016) and the second experiment carried out in 2017 is related to identify deep faults in the Roer Valley Graben. Both project are very relevant for this study and for the Netherlands as the 2015 experiment targeted the Lower Carboniferous Limestone Group and the 2017 experiment targeted deep faults, both to identify geothermal reservoirs.

The aim of the CSEM-MT survey conducted in 2015 was to investigate the potential of the methods to image deep geothermal resources in highly urbanized areas. A pre-survey 3D CSEM modelling was carried out to test different source configurations and select the optimal source-receiver offset. An a-priori resistivity model was based on the available resistivity logs. A total of nine MT/CSEM stations was acquired and a single 2x1 km orthogonal dipole was used as current source. Minimal and maximal distance between source and receiver where 6 and 12 km respectively. Due to the high levels of cultural noise, data processing required both extensive manual inspection of the time series and frequency domain processing. Out of the nine CSEM stations, two were too noisy to be useful. The QC of the processed MT data revealed that only one out of the nine stations was of sufficient data quality for all components (xy and yx) over the frequency bands of interest (0.01 Hz – 1 Hz).

Both CSEM and MT stations were 1-D inverted and compared to the available resistivity log of a nearby well. As shown in Figure 19, the 1-D resistivity profiles fit the log data of the MOL-GT borehole up to a depth of roughly 1,500 m and follow the trend of the resistivity reasonably well in the deeper part of the well. The average resistivities measured with MT and CSEM capture the subsurface resistivity well, but has problems imaging the actual depth of the resistivity interfaces, and has a much lower resolution.

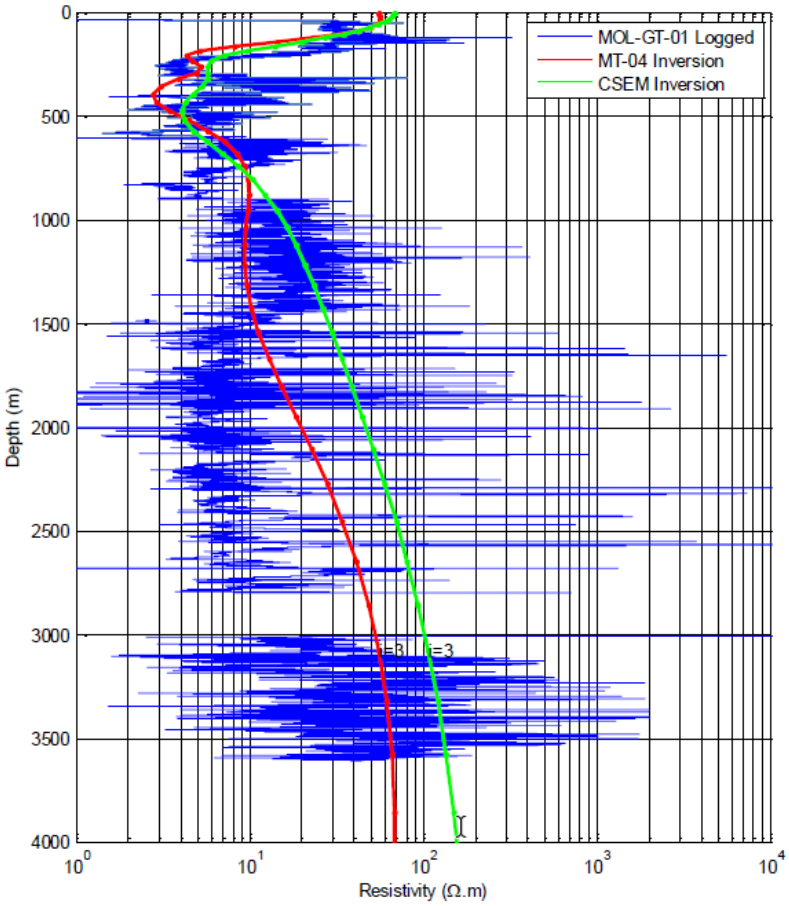

Figure 19 | 1-D resistivity profile of stations CSEM stations CS-04 and MT station MT-04 compared to the (high resolution) resistivity log in bore hole MOL-GT-01. The difference between the CSEM and the MT results is explained by the fact that thin conductive shale layers and thin resistive coal layers are present in the Upper Carboniferous and CSEM soundings are more sensitive to vertical resistivity variations, while MT soundings is more sensitive to horizontal resistivity variations (Coppo et al., 2016).

Details of the 2017 survey have not yet been published. By personal communication with VITO it was possible to identify the most important findings and lessons learnt from this combined CSEM-MT experiment (Lagrou, 2019). As shown in Figure 20, total of 60 stations was measured during the survey, 20 measuring the full -5 component- EM field and 40 measuring the horizontal electric field.

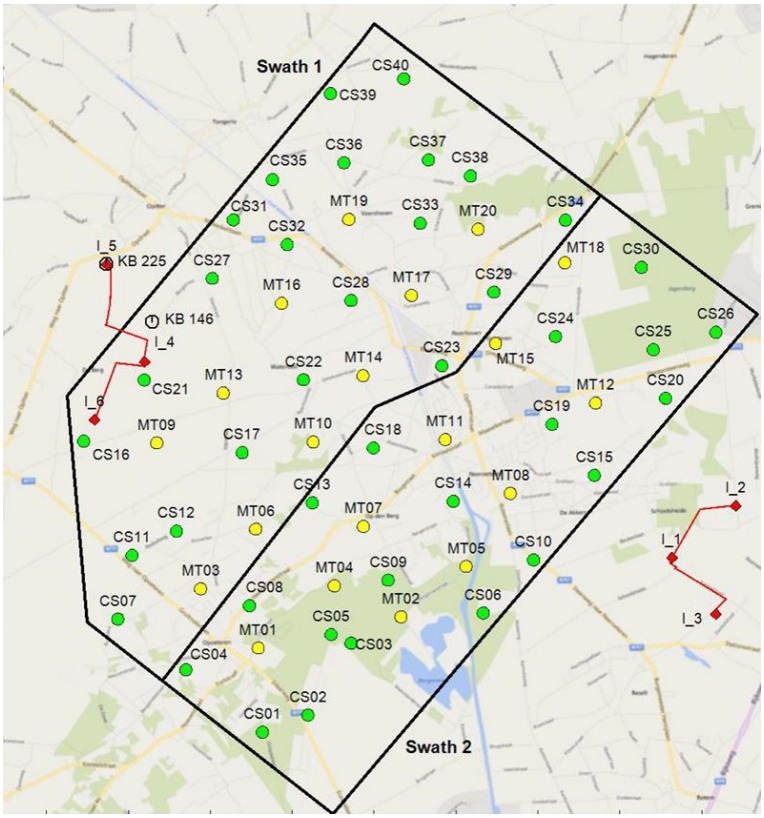

Figure 20 | Survey layout of the 2017 CSEM-MT survey. Shown are the full MT stations (yellow dots), the two component stations (green dots) and the injection points (red squares), source: (Lagrou, 2019).

One of the objectives of the experiment was to investigate the feasibility to use (the steel casings of) deep boreholes as current injection point. Due to high contact resistance and some HSE concerns, only one borehole was used. To create a dipole, the other injection points were regular ground electrodes. This setup was only used for swath 2.

As the survey area is densely populated for an EM survey, this experiment proved to be very challenging for the crew and equipment to carry out. As the shallow subsurface was very resistive, extra attention needed to be paid to the preparation of the injection dipoles. The presence of numerous noise source such as electrical fences, power lines, wind turbines and other infrastructure producing EM noise, caused reduced signal-to-noise ratios and produced significant challenges in data processing.

The main findings, based on the report delivered by CGG[3], of this experiment are the following:

- Up to depths of about 2 km, electromagnetic methods can be successfully applied. In terms of data quality and signal resolution, meaningful geological structures can imaged up to these depths.
- CSEM is a valuable method, complementary or prior to a seismic campaign.
- Measuring MT signal is very challenging in an urbanized environment.
- As a result of a roughly one kilometre thick conductive formation, it is difficult for the current to penetrate the resistive layers underneath.

[3] Not in the possesion of the author, but received from VITO.

The combined MT and CSEM pilot near Luttelgeest

To test the potential of EM methods as an exploration methodology for geothermal energy, a combined MT and CSEM pilot experiment was conducted near the village of Luttelgeest in the Noordoostpolder in 2017. The experiment was funded by the province of Flevoland and a group of greenhouse entrepreneurs. The experiment targeted the Slochteren Formation geothermal aquifer in which a geothermal system is realized (see Figure 21). A total of 17 CSEM and 6 MT stations were measured. A remote reference MT station was installed 20 km away at the Dwingelerveld, while a 1 km long CSEM transmitter dipole was installed in the southeastern corner of the survey area. The survey was designed such that the stations are aligned roughly parallel to the orientation of the 2-D seismic lines acquired in the area, one of the stations is located in the vicinity of the hydrocarbon well MKO-01-S1 as shown in Figure 21.

The two datasets were processed and inverted to determine the subsurface resistivity structure and investigate the applicability of MT and CSEM for geothermal exploration.

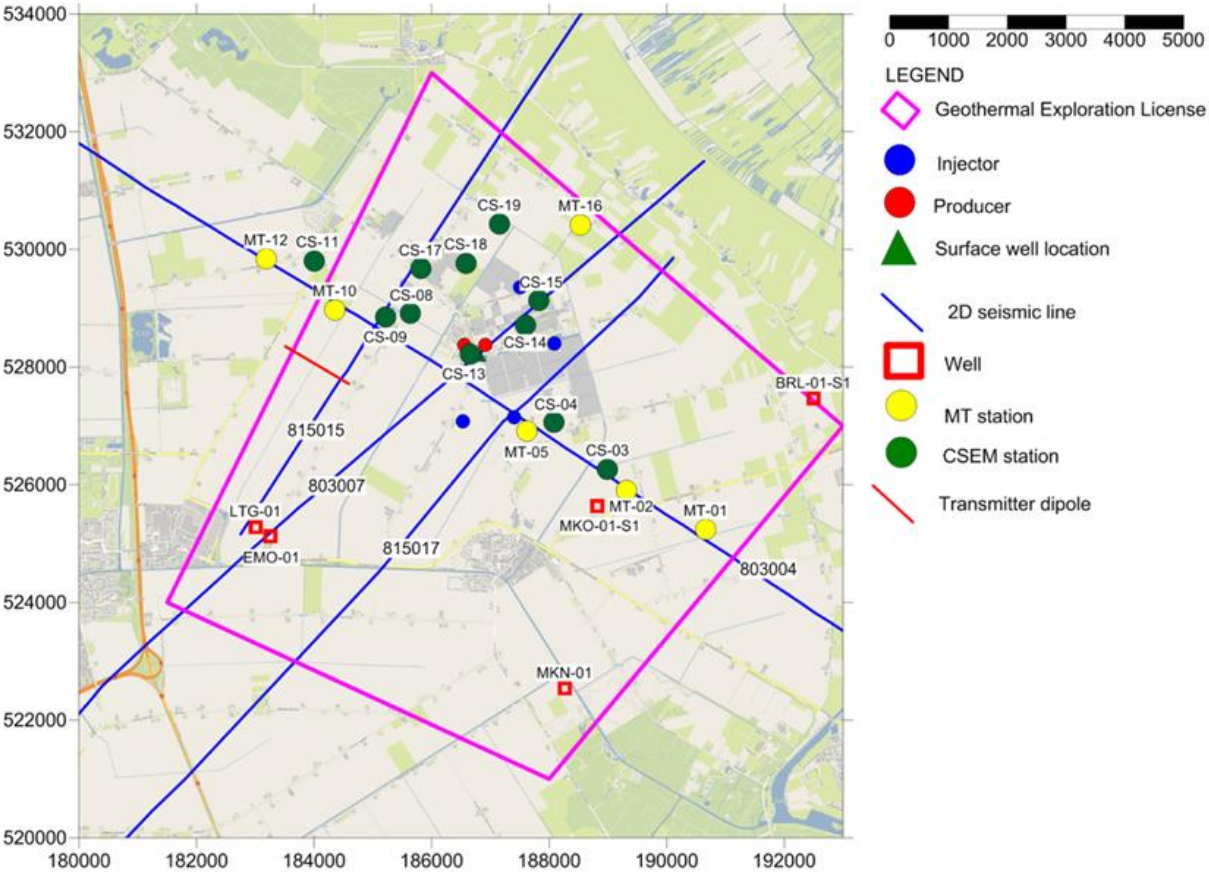

Figure 21 | Survey layout of the combined CSEM and MT pilot near Luttelgeest. MT stations (yellow) were also utilized as CSEM station when injecting current into the ground. MT stations are measuring five components of the EM field, while CSEM stations are measuring 2 components of the EM field. Also shown are hydrocarbon wells and the subsurface locations of the geothermal system.

Data processing

The recorded MT and CSEM data were processed using inhouse processing code, following the workflow and principles introduced in the Chapter “Electromagnetic data acquisition, processing and inversion”. An example of the MT time series data of the four horizontal components of the EM-field recorded at station MT-02 is shown in Figure 22. The data is recorded at 256 Hz and the 50 Hz signal generated by the high voltage power line in the

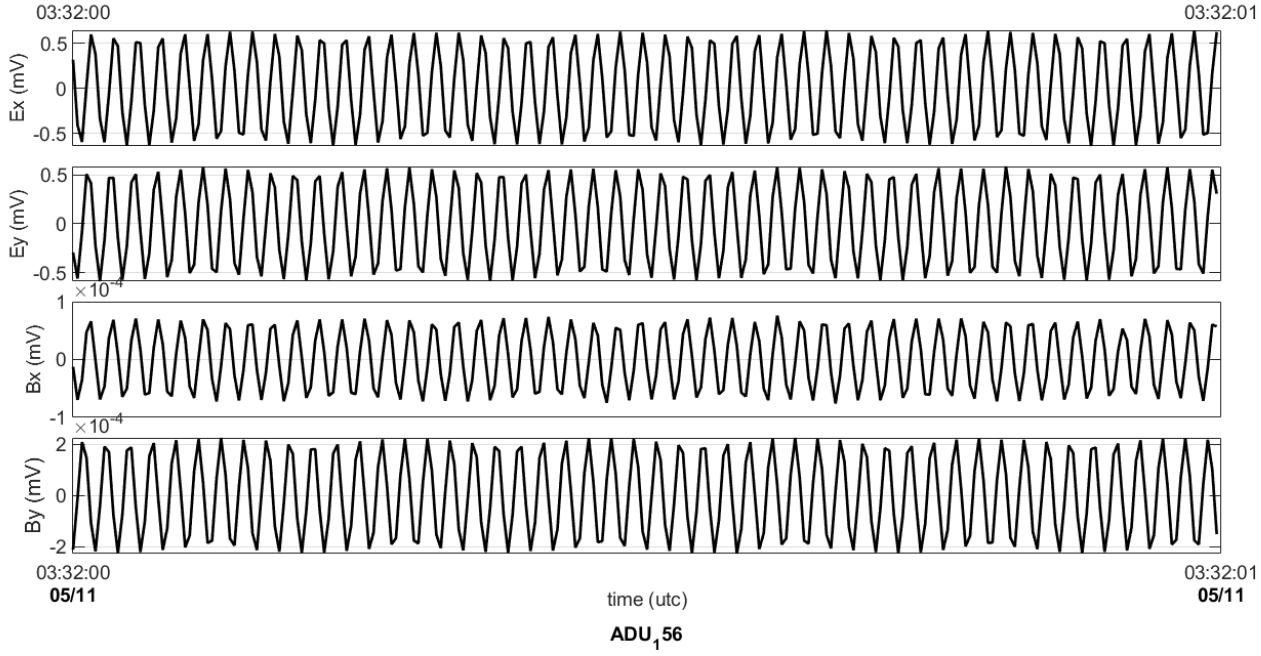

survey area is clearly visible. The same 50 Hz and its harmonics are also clearly visible in the power spectrum of station MT-02 as shown in Figure 23. In this figure it can be observed that the recorded signal is relatively noisy.

Figure 22 | One second of time series data recorded at 256 Hz by datalogger ADU_156 located at station MT-02. Visible is the 50 Hz signal caused by the high voltage power line near the survey area. Shown are all four recorded channels, from top to bottom these are the horizontal electric field in the x-direction, the horizontal electrical field in the y-direction, the horizontal magnetic field in the x-direction and the horizontal magnetic field in the y-direction.

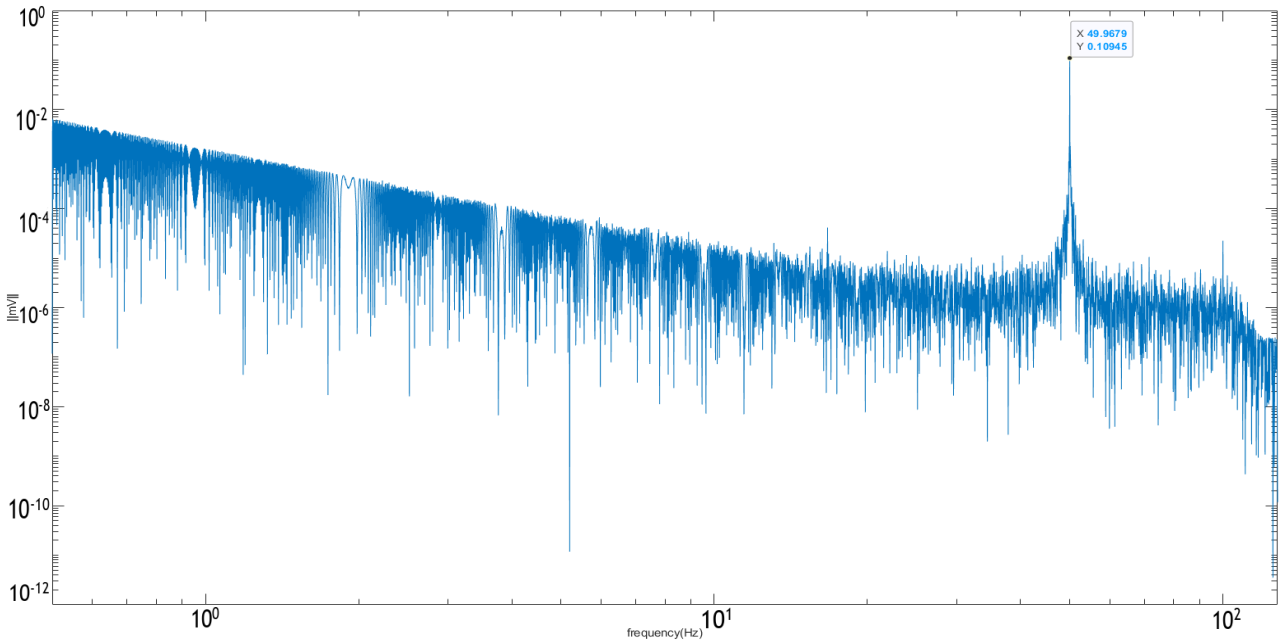

Figure 23 | Power spectrum of the recorded signal at station MT-02. Clearly visible is the 50 Hz peak from the high voltage power lines. Horizontal axis shows frequency in Hz between 0.5 and 200 Hz and vertical axis absolute values of the recorded amplitudes (10^{-12} – 1 ||mV||).

After processing, as listed in Table 22, it can be concluded that four of the six MT stations have a recorded a reasonable or good response, while two MT stations have recorded noisy data. One of these stations (MT-16) was located too close to the high voltage power line (< 200 m), while the noise source of the other station is unknown. An example of a good and a poor unedited station response is shown or stations MT-02 and MT-16 in Figure 11.

Table 2 | Overview of the quality of the recorded MT and CSEM data per injection frequency per station. For the CSEM stations, the distance to the dipole source is also given.

MT station	quality	CSEM station	quality[4]	Distance to dipole (m)
MT-01	reasonable	CS003	poor	5.204
MT-02	good	CS004	poor	4.099
MT-05	good	CS008	good	1.785
MT-10	good	CS009	good	1.396
MT-12	poor	CS011	good	1.787
MT-16	poor	CS013	poor	2.565
		CS014	unknown	3.570
		CS015	good	3.896
		CS017	reasonable	2.392
		CS018	good	3.040
		CS019	poor	3.896

[4] Quality per station is poor, the table gives an evaluation per injection frequency.

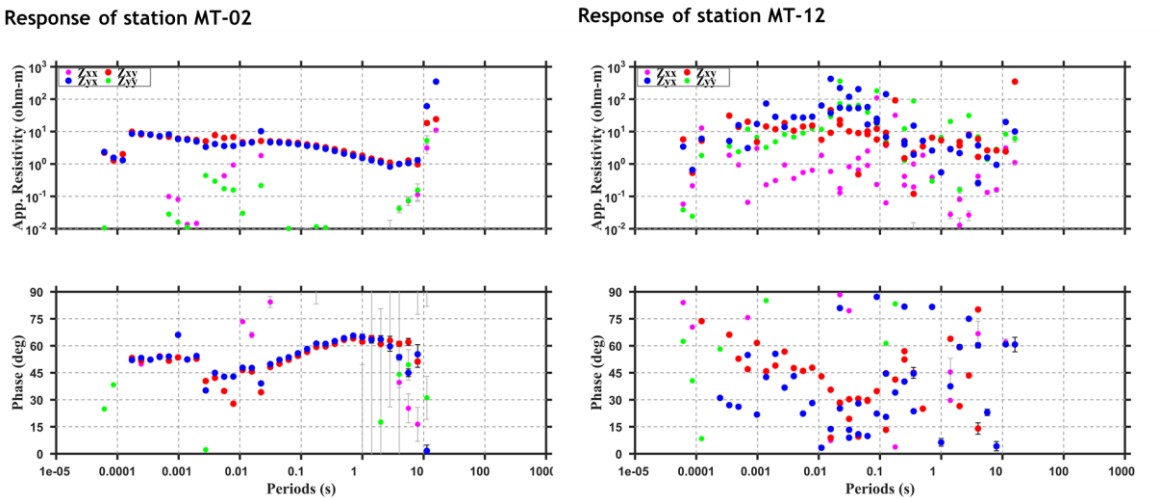

Figure 24 | Unedited station response of stations MT-02 (good data quality) and MT-12 (poor data quality).

In Figure 25 the time series data of CSEM station CS-009 and the source signal are shown. As with the MT data, the 50 Hz signal from the power line is clearly visible. The injected 0,5 Hz square waveform signal is clearly visible in the source signal. In the power spectrum of station CS-09, as shown in Figure 26, the removed 50 Hz signal of the power lines can be observed as negative peaks, while the injected frequencies and their harmonics are visible as positive peaks.

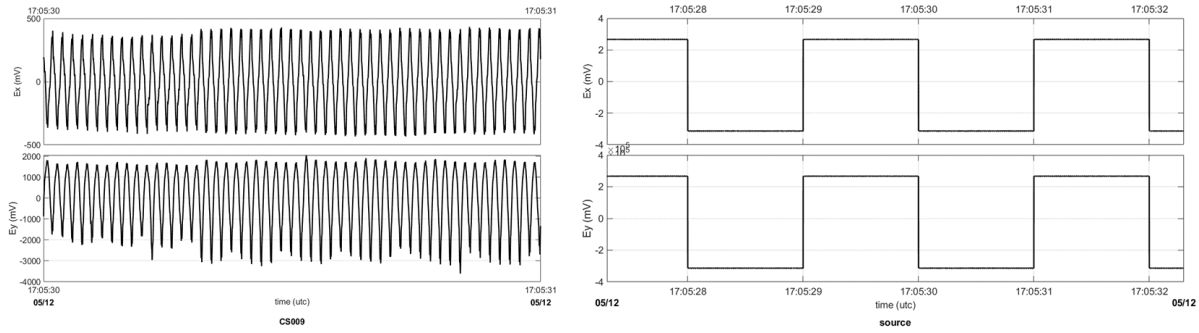

Figure 25 | Time series data of CSEM station CS-09 (1 sec) and the square waveform source signal (5,5 sec) injected with a cycle of 0,5 Hz. As with the recorded MT data the 50 Hz noise from the power line is clearly visible in the time series data.

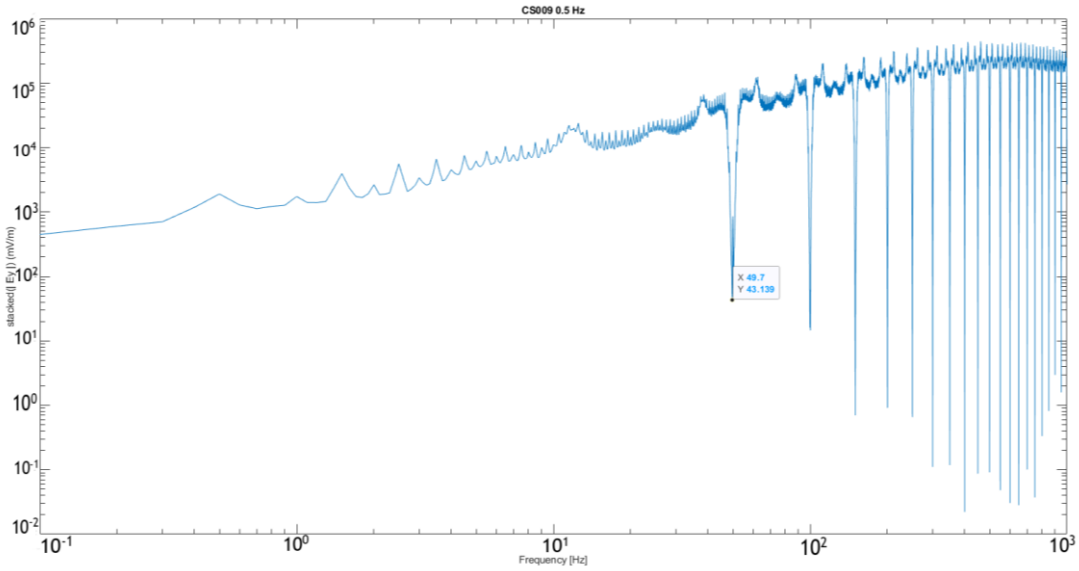

Figure 26 | Power spectrum of CSEM station CS-09. Clearly visible is the (filtered out) 50 Hz signal and its harmonics. Horizontal axis shows frequency in Hz and vertical axis absolute values of the recorded amplitudes.

During processing it became clear that there is a problem in the recorded data. Unfortunately, the source of this problem could not be reconstructed, resulting in unrealistic station responses. The processed station response of station CS-09 is shown in Figure 27. Where, as for MT data, in a realistic CSEM response all amplitudes and phases should -more or less- form a continuous smooth line, the amplitudes and phase response seems to be dependent on the injection frequency.

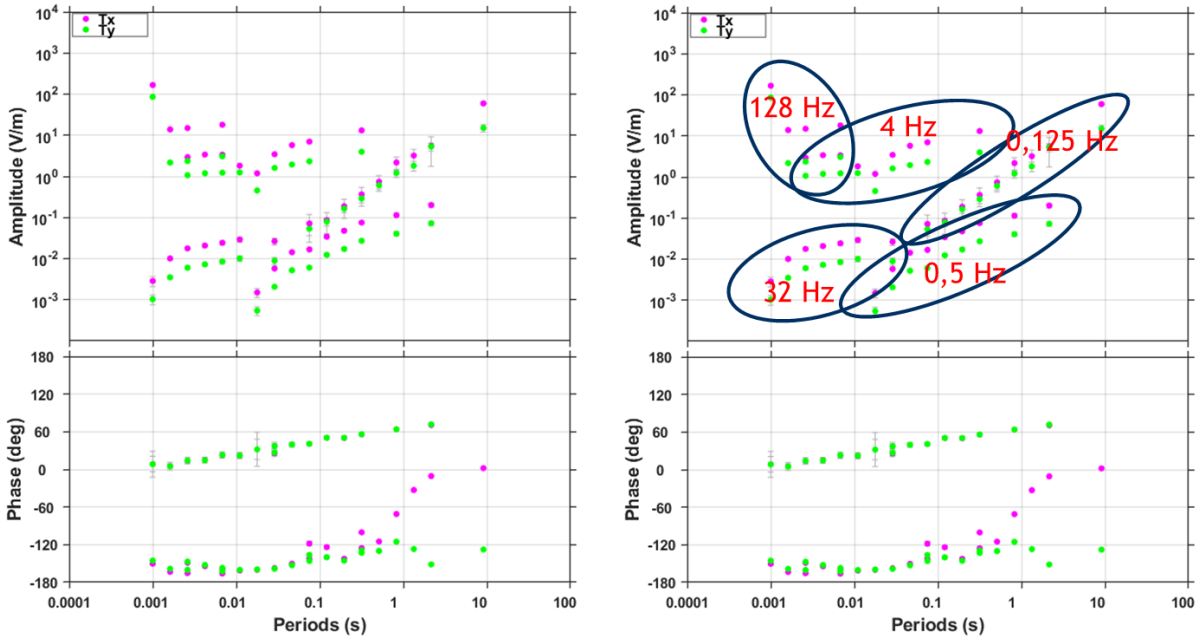

Figure 27 | Station response of CS-09 (both left and right panel). In the right panel, the responses of the various injection frequencies are indicated.

Although the resulting responses are not reliable, an qualitative assessment of the data quality was possible. The results of this are listed in Table 2 and an apparent correlation between distance to the source dipole and receiver was observed. Further examination showed that poor data quality was either recorded due to the presence of EM-noise in the vicinity of the location, or a result of source-receiver distances above 4 km.

Inversion

To be able to make a meaningful resistivity model of the subsurface, the MT responses need to be edited. Unreliable data points are masked before 1-D inversion to create a smooth MT transfer function. The data points masked are the result of either a weak MT signal or the recorded noise consequently, showing noise instead of data. As it turned out, recorded data with a period below approximately 0.03 s (33 Hz) are unreliable. Consequently, the maximum frequency range inverted is 33 Hz – 10 s (0.1 Hz). As a result, penetration depths of inversion models are limited. The 1-D inversion of the MT station recorded close to dry well MKO-01-S1 is shown in Figure 28. The 1-D inversion result shows that the penetration depth of this recording is approximately 1800.

The 1-D inversion result of station MT-02 and the smoothed ILD-log of well MKO-01-S1 are shown in Figure 29. Based on this Figure, it can be concluded that up to approximately 1500 m depth, the resistivity trends of 1-D layered model (red) and the well log data correlate. Overall the resistivity values of the 1-D inversion model are realistic. With more sophisticated software, a better result might be achieved.

The responses of MT stations MT-01, MT-05 and MT-10 were also 1-D inverted. Unfortunately, the model results of these inversion are either unrealistic, showing high resistivities at shallow depth or have a very limited penetration depth. The model fit is computed as RMS and are for all inverted models between 2 and 5.

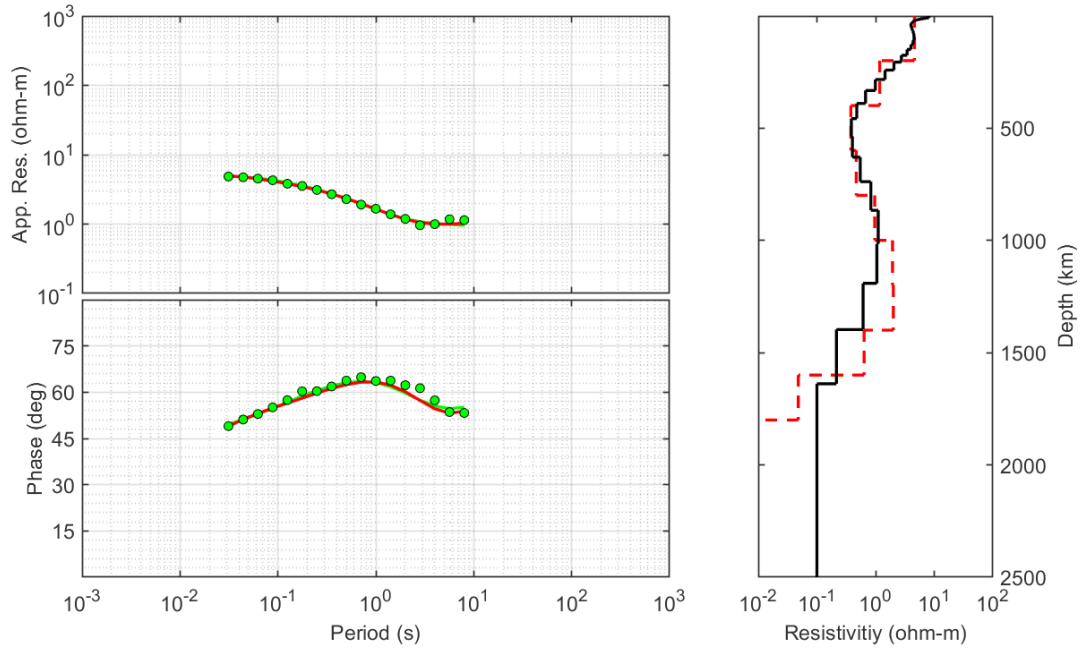

Figure 28 | Inversion result of station MT-02. Left upper panel, apparent resistivity versus period, left lower panel, phase versus period. Green dots show the invariant of the observed data, red line the 1-D layered inversion model. Right panel shows the 1-D inversion model. Black line is the smooth Occam inversion, red dashed line is the 1-D layered model inversion.

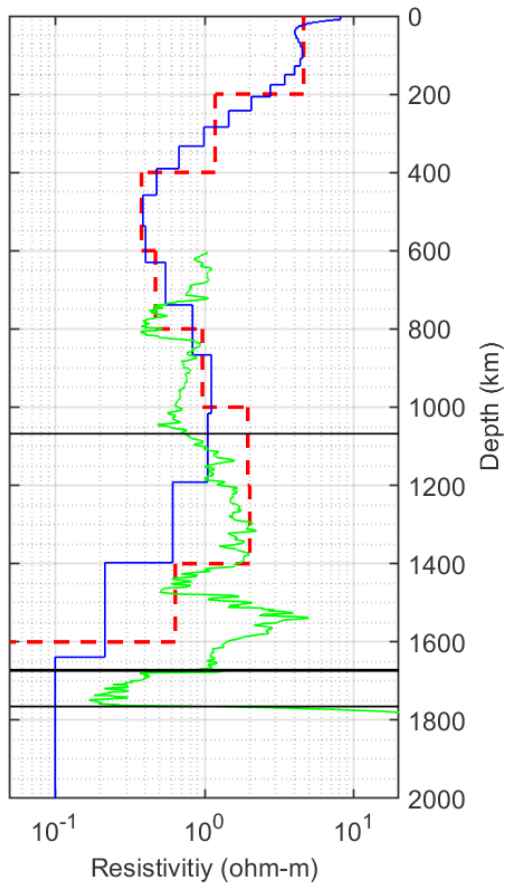

Figure 29 | 1-D inversion result of station MT-02. Red: layered model; Black: Occam model; Green: Smoothed ILD-log of well MKO-01-S1. Black horizontal lines from top to bottom: Base North Sea; Top Slochteren; Base Slochteren.

An attempt was made to invert the CSEM response of station CS-009 for the responses corresponding to the injected signal at 0.125 Hz and 32 Hz. Before running the inversion a forward synthetic model was created as shown in Figure 30. This response is based on the resistivities as observed in well MKO-01-S1.

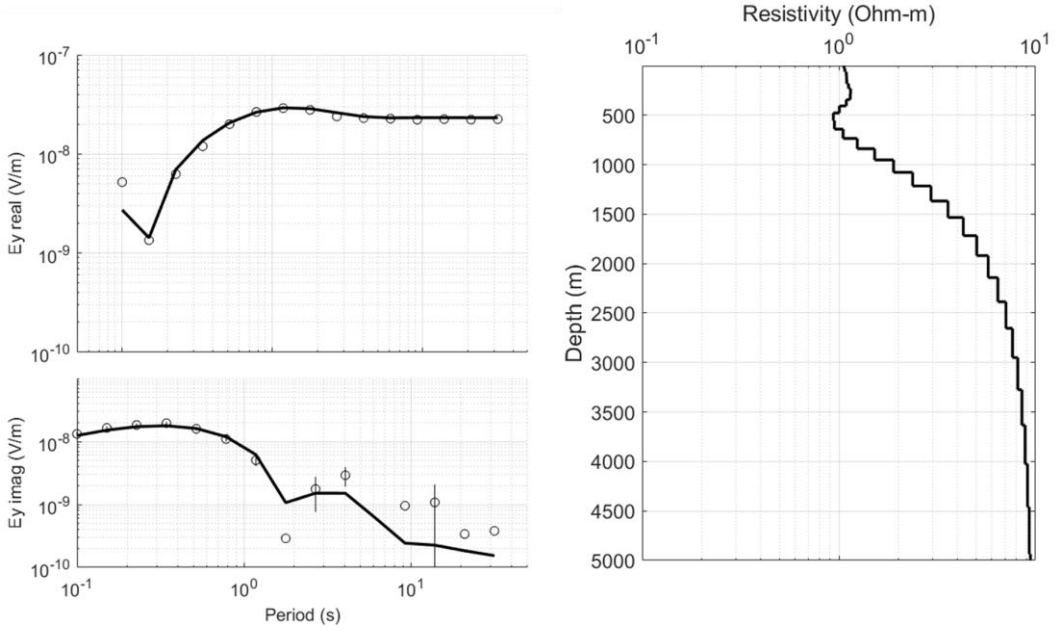

Figure 30 | Forward model response of CSEM station CS-09. Left upper panel shows the real part of the modelled Ey response and left lower panel shown the imaginary part of the modelled Ey response. Right panel shows the resulting 1-D inversion model.

As it turned out, the values of the responses of the CSEM stations are unrealistically high, and also inconsistent. This makes it hard to create a meaningful model. The best result is shown in Figure 31. As can be observed here, modelled resistivity values are unrealistically high and there is a large misfit between observed and modelled data.

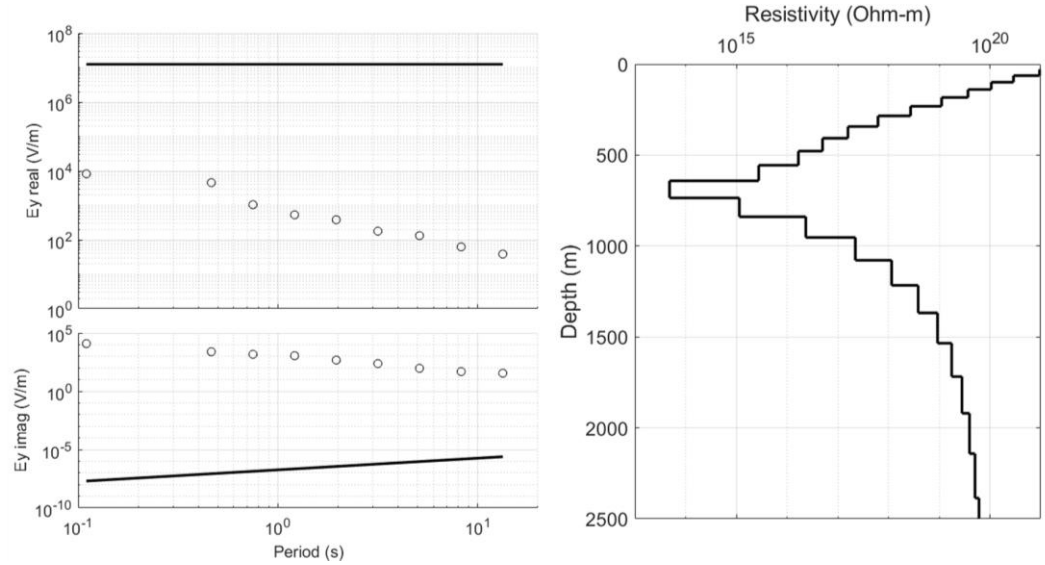

Figure 31 | 1-D inversion model of CSEM station CS-09. Left upper panel shows the real part of the observed (dots) and modelled Ey response and left lower panel shown the imaginary part of the observed (dots) and modelled Ey response. Right panel shows the resulting 1-D inversion model.

Conclusions

Since the data processing is hampered by a data issue, this case study is for the feasibility of the CSEM method for geothermal exploration not representative for the Dutch case. Based on the data recording, data processing and data inversion of the combined MT-CSEM experiment near Luttelgeest the following is concluded:

- Good quality MT data can be recorded, however long periods of good quality signal are necessary and data needs to be recorded continuously – which was not the case here.
- In this survey layout and recording time, a maximum depth of about 1800 m can be achieved using MT.
- It is expected that better inversion results can be obtained when using commercial software.
- Good quality CSEM data can be recorded.
- Unfortunately, due to a data problem, the data was not processed properly and unrealistic inversion results were obtained.
- The 1-D synthetic model indicates that a depth of approximately 3000 m.
- It is expected that better processing results of the CSEM data can be achieved when using the inhouse CGG-code.

The CSEM experiment at the Schoonebeek oil field

In 2014 a CSEM field experiment was conducted at the Schoonebeek oil field in the east of the Netherlands (Schaller, 2018) as shown in Figure 32. The goal of the experiment was to investigate if the steam front of the steam injected into the oil reservoir for enhanced oil recovery could be monitored. Although not aimed at geothermal and with a relatively shallow target of 700 to 800 m, this is one of the few well-documented examples of land-based CSEM deployed in the Netherlands.

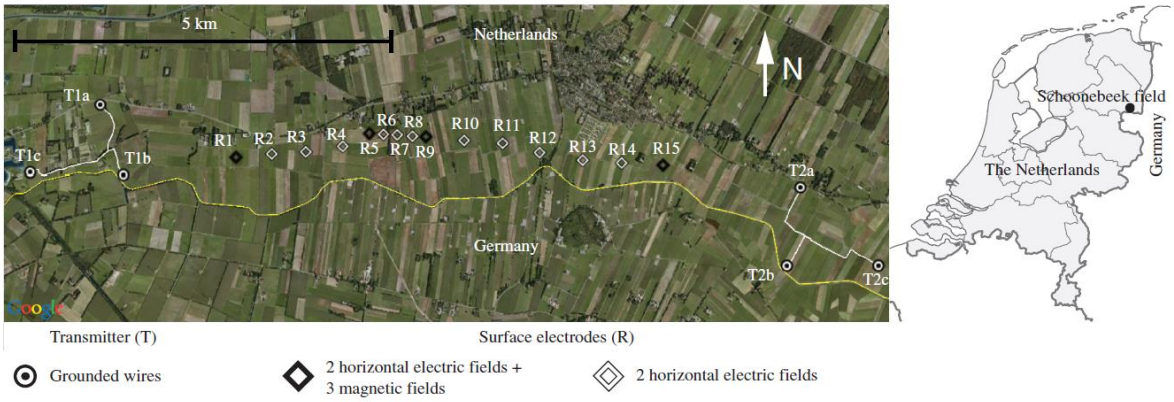

Figure 32 | Survey layout of the CSEM experiment at the Schoonebeek oil field (from Schaller et al., 2018).

A forward modelling study was carried out to design the optimal acquisition field setup capable of resolving the resistive reservoir target zone in high resolution. This modelling study showed that small electrical resistive structures can be detected, but that their absolute dimensions and accurate resistivities are difficult to determine.

The experiment proved that with a single receiver line of 15 receivers and using two inline transmitters, as shown in Figure 32 at a depth around 800 m, it is possible to resolve a resistivity distribution inside a reservoir formation (Schaller et al., 2018). Additionally, resistive and conductive features initiated by injected fluids are observed in the acquired data.

An important finding from this study is that 1-D inversion is capable of recovering accurate reservoir depth, while small resistive anomalies and lateral variations could not be resolved.

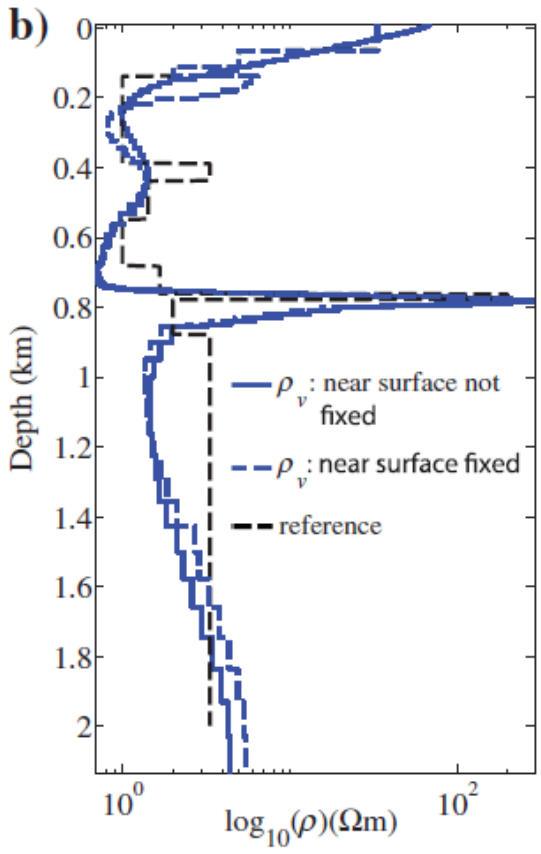

Figure 33 | 1-D resistivity model of the Schoonebeek experiment. Black dashed reference line is the resistivity structure of the subsurface based on well log information. Blue lines show two different 1-D resistivity models - with fixed and without fixed near surface resistivity layers – based on the acquired CSEM data. The highly resistive reservoir is clearly visible around 800 m depth. (From Schaller et al., 2018).

Practical considerations for acquiring EM data in the Netherlands

Cultural noise

The Netherlands is a country with numerous cultural EM sources, such as, for example, electric fences, corrosion protected pipes, subsurface cables, DC railway network, water pumps, etc.. This will always be a challenge when acquiring EM data. Experiments indicate that it is possible to acquire good quality MT and CSEM data at relatively quiet, rural locations. It is unlikely that CSEM and MT as an geothermal exploration method can be deployed successfully in urbanized areas. Furthermore, it is a disadvantage that the Dutch railway system is a DC system which implies that trains are moving EM sources which disturb the recorded EM signal. In practice, the EM signal from the train doesn't travel far due to the conductive subsurface, although a minimum distance of an MT station from a DC railway of approximately 5 km[5] is suggested. An EM station can probably be located at a closer distance from a DC railway.

[5] A test survey which potentially can confirm this number was carried out, but this data was not found during this study.

In Figure 34 the implications of a 5 km contour around the DC railway systems for the available area where an EM survey can be conducted, is illustrated.

Figure 34 | Railway map of the Netherlands with a 5 km contour in orange around all dc electrified railways. The circles represent small industry related dc railway systems.

Subsurface: what can you expect?

Being a sedimentary basin the subsurface of the Netherlands is electrically very conductive for the first kilometre and in some regions even up to depths of four kilometre or more. The water filled sand layers and clay layers have little conductivity contrast which makes distinguishing lithological boundaries challenging. Additionally, as the aim of a geothermal exploration would be a highly conductive structure, resolving it using MT might impose problems (see Figure 35). As MT is typically strong in resolving conductive structures, given its composition, the Dutch subsurface will be hard to image. As CSEM is using a source, it is strong in resolving resistive structures, it offers more potential when imaging the Dutch subsurface.

	Model 4.2
NU	7.4
N	4.0
CK	2.6
KN	1.6
DCC	8.8
DC	50.0
CL	300.0
OB	67.4
Basement	300.0

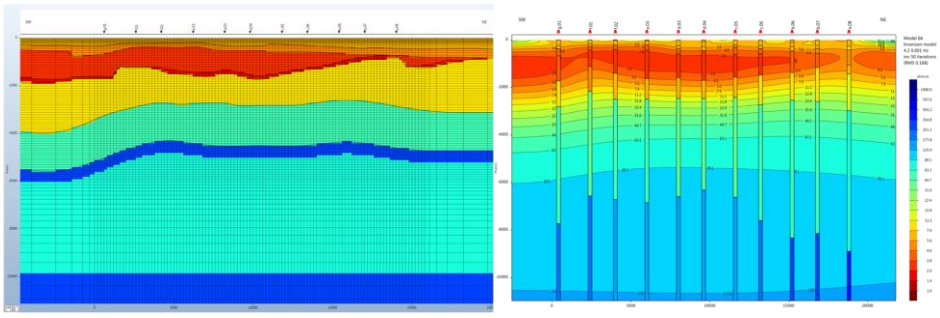

Figure 35 | Synthetic resistivity model of the Dutch subsurface. From left to right, (left) average exploration well based electrical resistivities for the different geological groups in the Netherlands in the area of Nijmegen. (middle) 2-D initial resistivity model of the Dutch subsurface in the area of Nijmegen including MT stations on the surface. (right) Resistivity model based on the synthetic EM responses of the MT stations of the initial resistivity model. It is observed that up to the Dinantian Carbonates (CL), the input resistivities and structures are reasonably resolved, while depth of the top CL is positioned too deep. Below the top CL no resistivity contrasts are detected. Horizonal axis of the model spans roughly 22 km, vertical axis of the two models are between 0 and 11 km depth in steps of 2000 m and resistivity scales are similar for all three models; red is conductive, blue is resistive (van Aken, 2016).

To explore the resolving potential of the magnetotelluric method, a synthetic resistivity model of the subsurface was created by van Aken (2016). The initial subsurface resistivity model is based on the California geothermal project. Besides a basecase, which is not presented here, two cases were investigated. The background resistivity model consists of a resistive base, the Dinantian Carbonates, overlain by more conductive layers. Resistivities of these layers were based on resistivity measurements in nearby wells. Two cases were modeled, one with an electrically conductive vertical fault and a reservoir (Figure 36, left), and one with a only a reservoir and no fault (Figure 36, right). As can be observed in Figure 36, the resulting resistivity models, the synthetic model is able to the resolve the presence of the reservoir at a too shallow depth, but is not able to image fault. It must be noted that this was a very basis experiment, which has can be optimized, e.g. by using a more accurate initial model, optimized parameterization, station locations, or using a 3-D approach.

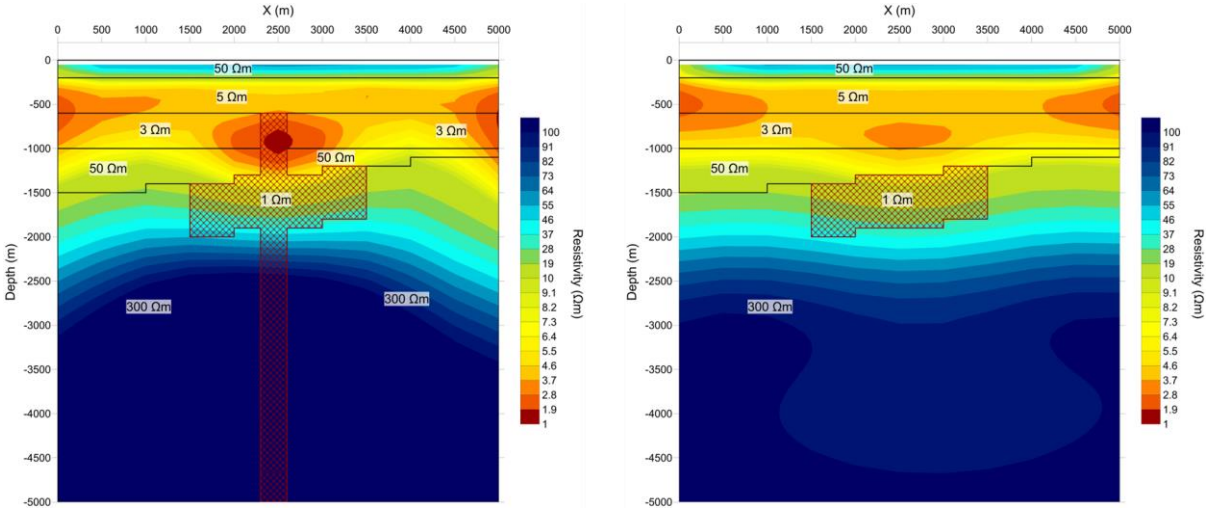

Figure 36 | Synthetic 2-D resistivity model based on the conceptual model of the California geothermal project. Block model on the foreground shows the initial resistivity model, coloured model shown the resulting resistivity model based on the data generated by the initial model. Left: reservoir and fault. Right: only reservoir.

Joint interpretation

As the result of a EM inversion is non-unique, a priori geological constraints can be added to the starting model to guide the inversion. In the Netherlands, this is especially useful in the depth interval where good quality interpreted seismic data is available. By using the structures, interpreted in the seismic data, the starting resistivity model and, if possible, assigning resistivities to them, the model solution has less freedom and is expect to be more realistic and contain more detail. Several examples of this type of joint inversion are published (e.g. Bujakowski et al., 2010; Muñoz et al., 2010).

Conclusions and recommendations

Learning from Dutch cases

Based on the examples discussed in this Chapter, the following factors that play an important role for applying MT or CSEM in the Netherlands are listed.

- The experiments in Luttelgeest and Belgium proved that with the EM method you can measure up to a depth of about 2 km below the surface.
- The experiments in Luttelgeest and Belgium proved that acquiring good quality EM data in Belgium and the Netherlands is possible, despite the numerous EM noise sources.
- It is important to design your survey and create a forward model of the target area either using MT or CSEM. This was an important difference between the success of the Luttelgeest and Schoonebeek cases. Insight in which structures can be resolved and which acquisition parameters are necessary for an optimal result, are crucial for a successful campaign.
- Experience from the pilot study, learned that pre-survey scouting of the area for non-visible EM sources is also necessary. Additionally, good communication with the land owners is necessary to make sure all potential noise sources are switched off and all permits for access to land are granted. This experiment also showed that impact of the DC railway network on the data quality is much smaller than anticipated.
- The pilot survey and the Luttelgeest experiment showed that the quality of the remote reference station impacts the survey results.
- Although not favourable for geothermal, the Schoonebeek and the Ten Broek cases clearly demonstrated that the CSEM/CSAMT methods can resolve shallow (up to 1,000 m depth) resistive geological structures of various shapes.
- Not directly expected, but the Luttelgeest experiment showed that EM noise also plays a significant role in CSEM data quality.
- In a survey area with a size comparable to the Luttelgeest experiment, using one dipole utilizing a maximum source-receiver-distance of 4 km, is not optimal. Better results are expected when locating two or three dipoles around the survey area.
- The synthetic experiments showed that when modelling, information from wells and seismic data should be used to build realistic subsurface resistivity models.
- In the case of the survey near Mol, the geothermal reservoir is visible in the MT-CSEM data.
- The examples discussed here, illustrate that CSEM and MT offer potential for shallow exploration in area’s with limited (2-D) seismic data for conventional geothermal exploration.
- The surveys in Belgium demonstrated that interpreted CSEM and/or MT data can be a valuable extra source of information which may help in determine depth and dimension of the geothermal reservoir, in addition to seismic and well log data.

Recommendations for a successful electromagnetic field campaign

Based on the learnings discussed above, the following recommendations are made for the successful conductance of an electromagnetic field campaign:

- Prepare! Scouting planned survey locations for potential noise sources and optimizing them is the easiest route to acquiring good quality data. Ensure you have access to all the planned sites by a permitting campaign. Furthermore scout and test, if possible, several remote reference locations. Superb data quality of the remote reference station improves data quality significantly. If possible, plan the survey during a period with a predicted high Kp-index.
- Choose a target that can be detected in the electromagnetic data, there should be a detectable resistivity contrast between the target and the surrounding rocks. To do this, make synthetic models to predict the subsurface response and determine to optimal survey parameters and layout. Use existing knowledge and data (seismic and well data) from the subsurface to do this.
- Stay away from urbanized areas when planning a survey. Don’t plan a station location too close to a DC railway line.
- Before you start the actual survey, check and prepare all your survey equipment: data loggers, source, coils and electrodes.
- In the field, plan and be pragmatic to obtain the best survey results. Stay on top of your crew. Solid field procedures are very important for good quality data.
- During processing, take time and test various processing strategies. Due to the presence of EM-noise and the subsurface conditions, thoughtful processing is necessary in the Netherlands.
- During inversion modelling, use geological constraints from existing subsurface models and well log data to guide the inversion modelling. This increases the accuracy and reliability of the resulting subsurface model.
- As the electromagnetic response measured is a volumetric measurement, more reliable results are obtained by 3-D models. The validity structures observed in the 3-D model can be tested by stitched or interpolated 1-D models.

References

Árnason, K., Eysteinsson, H., Hersir, G.P., 2010. Joint 1D inversion of TEM and MT data and 3D inversion of MT data in the Hengill area, SW Iceland. Geothermics 39, 13–34. https://doi.org/10.1016/j.geothermics.2010.01.002

Boxem, T.A.P., Veldkamp, J.G., Van Wees, J.D., 2016. Ultra-diepe geothermie: overzicht, inzicht & to-do ondergrond (No. B.5120.04). TNO.

Bujakowski, W., Barbacki, A., Czerwińska, B., Pająk, L., Pussak, M., Stefaniuk, M., Trześniowski, Z., 2010. Integrated seismic and magnetotelluric exploration of the Skierniewice, Poland, geothermal test site. Geothermics 39, 78–93. https://doi.org/10.1016/j.geothermics.2010.01.003

Chave, A.D., Jones, A.G., 2012. The Magnetotelluric Method. Cambridge University Press.

Chave, A.D., Thomson, D.J., 2004. Bounded influence magnetotelluric response function estimation. Geophysical Journal International 157, 988–1006. https://doi.org/10.1111/j.1365-246X.2004.02203.x

Chave, A.D., Thomson, D.J., Ander, M.E., 1987. On the robust estimation of power spectra, coherences, and transfer functions. J. Geophys. Res. 92, 633. https://doi.org/10.1029/JB092iB01p00633

Constable, S., 2010. Ten years of marine CSEM for hydrocarbon exploration. GEOPHYSICS 75, 75A67-75A81.

Constable, S., Srnka, L., 2007. An introduction to marine controlled-source electromagnetic methods for hydrocarbon exploration. GEOPHYSICS, Special Section — Marine Controlled-Source Electromagnetic Methods 72, WA3–WA12. https://doi.org/10.1190/1.2432483

Coppo, N., Darnet, M., Harcouet-menou, V., Manzella, A., Romano, G., Wawrzyniak, P., Lagrou, D., Girard, J.F., 2016. Characterization of Deep Geothermal Energy Resources in Low enthalpy sedimentary basins in Belgium using Electro-Magnetic Methods – CSEM and MT results. European Geothermal Congress 2016.

Cumming, W., Mackie, R., Geoscience, C., 2010. Resistivity Imaging of Geothermal Resources Using 1D, 2D and 3D MT Inversion and TDEM Static Shift Correction Illustrated by a Glass Mountain Case History, in: Proceedings World Geothermal Congress 2010. Presented at the World Geothermal Congress, Bali, Indonesia, p. 10.

Delhaye, R., Rath, V., Jones, A.G., Muller, M.R., Reay, D., 2019. Quantitative geothermal interpretation of electrical resistivity models of the Rathlin Basin, Northern Ireland. Geothermics 77, 175–187. https://doi.org/10.1016/j.geothermics.2018.09.012

den Boer, E., Eikelboom, J., van Driel, P., Watts, D., 2000. Resistivity imaging of shallow salt with magnetotellurics as an aid to prestack depth migration. First Break 18, 19–26. https://doi.org/10.1046/j.1365-2397.2000.181047.x

Egbert, G.D., Booker, J.R., 1986. Robust estimation of geomagnetic transfer-functions. Geophys. J. R. Astr. Soc. 87, 173–194.

Egbert, G.D., Kelbert, A., 2012. Computational recipes for electromagnetic inverse problems: Computational recipes for EM inverse problems. Geophysical Journal International 189, 251–267. https://doi.org/10.1111/j.1365-246X.2011.05347.x

Erdogan, E., Candansayar, M.E., 2017. The conductivity structure of the Gediz Graben geothermal areaextracted from 2D and 3D magnetotelluric inversion: Synthetic andfield data applications. Geothermics 65, 170–179.

Flovenz, Ó., Spangenberg, E., Kulenkampff, J., Árnason, K., Karlsdóttir, R., Huenges, E., 2005. The Role of Electrical Interface Conduction in Geothermal Exploration, in: Proceedings World Geothermal Congress 2005. Presented at the World Geothermal Congress 2005, Antalya, Turkey.

Gamble, T.D., 1979. Magnetotellurics with a remote magnetic reference. Geophysics 44, 53–68. https://doi.org/10.1190/1.1440923
Hersir, G.P., Árnason, K., Vilhjálmsson, A.M., Saemundsson, K., Ágústsdóttir, Þ., Friðleifsson, G.Ó., 2018. Krýsuvík high temperature geothermal area in SW Iceland: Geological setting and 3D inversion of magnetotelluric (MT) resistivity data. Journal of Volcanology and Geothermal Research.
Junge, A., 1996. Characterization of and correction for cultural noise. Surveys in Geophysics 361–391.
Lagrou, D., 2019. lessons learned CSEM-MT campaign.
Larsen, J.C., Mackie, R.L., Manzella, A., Fiordelisi, A., Rieven, S., 1996. Robust smooth magnetotelluric transfer functions. Geophysical Journal International 801–819.
Ledo, J., Queralt, P., Martí, A., Jones, A.G., 2002. Two-dimensional interpretation of three-dimensional magnetotelluric data: an example of limitations and resolution. Geophysical Journal International 150, 127–139. https://doi.org/10.1046/j.1365-246X.2002.01705.x
Manzella, A., Spichak, V., Pushkarev, P., Sileva, D., Oskooi, B., Ruggieri, G., Sizov, Y., 2006. Deep Fluid Circulation in the Travale Geothermal Area and Its Relation with Tectonic Structure Investigated by a Magnetotelluric Survey, in: PROCEEDINGS, Thirty-First Workshop on Geothermal Reservoir Engineering. Presented at the Thirty-First Workshop on Geothermal Reservoir Engineering, Stanford, California, US, p. 6.
Muñoz, G., Bauer, K., Moeck, I., Schulze, A., Ritter, O., 2010. Exploring the Groß Schönebeck (Germany) geothermal site using a statistical joint interpretation of magnetotelluric and seismic tomography models. Geothermics 39, 35–45. https://doi.org/10.1016/j.geothermics.2009.12.004
Pellerin, L., Johnston, J., Hohmann, G., 1996. A numerical evaluation of electromagnetic methods in geothermal exploration. GEOPHYSICS 61, 121–130.
Schaller, A., 2018. Land time-lapse CSEM Collecting, modeling and inversion of CSEM data for a steam-injected oil field (Phd Thesis). TU Delft, Delft.
Schaller, A., Streich, R., Drijkoningen, G., Ritter, O., Slob, E., 2018. A land-based controlled-source electromagnetic method for oil field exploration: An example from the Schoonebeek oil field. Geophysics 83, WB1–WB17. https://doi.org/10.1190/geo2017-0022.1
Simpson, F., Bahr, K., 2005. Practical Magnetotellurics. Gottingen.
Siripunvaraporn, W., 2012. Three-Dimensional Magnetotelluric Inversion: An Introductory Guide for Developers and Users. Surv Geophys 33, 5–27. https://doi.org/10.1007/s10712-011-9122-6
Spichak, V., Manzella, A., 2009. Electromagnetic sounding of geothermal zones. Journal of Applied Geophysics 68, 459–478. https://doi.org/10.1016/j.jappgeo.2008.05.007
Spies, B.R., 1989. Depth of investigation in electromagnetic sounding methods. GEOPHYSICS 54, 872–888. https://doi.org/10.1190/1.1442716
Sternberg, B.K., Washburne, J.C., Pellerin, L., 1988. Correction for the static shift in magnetotellurics using transient electromagnetic soundings. GEOPHYSICS 53, 1459–1468. https://doi.org/10.1190/1.1442426
Streich, R., 2015. Controlled-Source Electromagnetic Approaches for Hydrocarbon Exploration and Monitoring on Land. Surveys in Geophysics. https://doi.org/10.1007/s10712-015-9336-0
Streich, R., Becken, M., Ritter, O., 2013. Robust processing of noisy land-based controlled-source electromagnetic data. Geophysics 5, E237–E247. https://doi.org/doi/10.1190/GEO2013-0026.1

Szarka, L., 1988. Geophysical aspects of man-made electro-magnetic noise in the earth - a review. Surveys in Geophysics 287–318.
van Aken, F., 2016. Geothermal exploration of the Lower Carboniferous Limestone Group in the Netherlands: A synthetic experiment using magnetotellurics (Msc thesis). VU Amsterdam.
van Leeuwen, W.A., 2016. Geothermal Exploration using the Magnetotelluric Method (Phd Thesis). Universiteit Utrecht, Utrecht.
van Leeuwen, W.A., Suryantini, Hersir, G.P., 2016. Quantitative comparison of two 3-D resistivity models of the Montelago geothermal prospect. IOP Conf. Ser.: Earth Environ. Sci. 42, 012029. https://doi.org/10.1088/1755-1315/42/1/012029

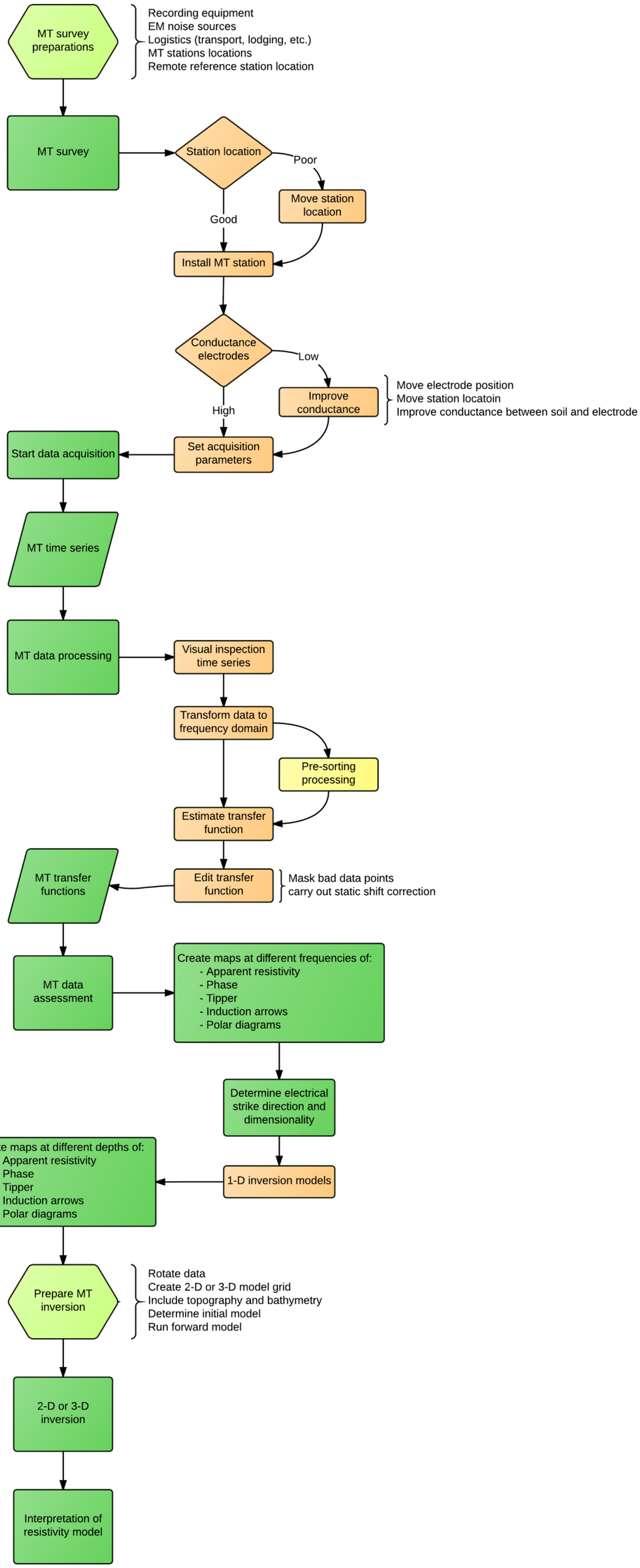
MT survey preparations
Recording equipment
EM noise sources
Logistics (transport, lodging, etc.)
MT stations locations
Remote reference station location
MT survey
Station location
Poor
Move station location
Good
Install MT station
Conductance electrodes
Low
Improve conductance
Move electrode position
Move station locatoin
Improve conductance between soil and electrode
High
Set acquisition parameters
Start data acquisition
MT time series
MT data processing
Visual inspection time series
Transform data to frequency domain
Pre-sorting processing
Estimate transfer function
MT transfer functions
Edit transfer function
Mask bad data points
carry out static shift correction
MT data assessment
Create maps at different frequencies of:
- Apparent resistivity
- Phase
- Tipper
- Induction arrows
- Polar diagrams
Determine electrical strike direction and dimensionality
Create maps at different depths of:
- Apparent resistivity
- Phase
- Tipper
- Induction arrows
- Polar diagrams
1-D inversion models
Prepare MT inversion
Rotate data
Create 2-D or 3-D model grid
Include topography and bathymetry
Determine initial model
Run forward model
2-D or 3-D inversion
Interpretation of resistivity model

This page intentionally left blank

Daalsesingel 1
3511 SV Utrecht
scan@ebn.nl
www.scanaardwarmte.nl

Onderzoek in de ondergrond voor aardwarmte